A MOLECULAR DYNAMICS STUDY ON CELLULOSE FIBER REINFORCED NANOCOMPOSITE

By

SHI LI

A THESIS PRESENTED TO THE GRADUATE SCHOOL
OF THE UNIVERSITY OF FLORIDA IN PARTIAL FULFILLMENT
OF THE REQUIREMENTS FOR THE DEGREE OF
MASTER OF SCIENCE

UNIVERSITY OF FLORIDA

2011

To my father and mother who have always supported me in all that I have done

ACKNOWLEDGMENTS

I would first and foremost like to thank my graduate advisor Dr. Youping Chen for supporting me with a funded and sponsored project and for her valuable insights and patience with we faced our challenges.

Special thanks to my graduate committee: Dr. Peter Ifju and Dr. Gary Peter for their willingness to review my work.

Thanks also to my fellow PhD students and friends: Qian Deng, Liming Xiong, Ning Zhang, Shengfeng Yang and Yongtao Li in Atomistic and Multiscale Mechanics group at the University of Florida for their invaluable comments during my time as part of the group. Extra thanks go to Qian Deng for his guidance and comments during the research. Special thanks to Brad LaCroix for his willingness to revise my thesis.

My utmost gratitude is to my parents. Thanks for their supporting and encouraging me throughout college and graduate school.

TABLE OF CONTENTS

page

LIST OF TABLES

LIST OF FIGURES

Abstract of Thesis Presented to the Graduate School
of the University of Florida in Partial Fulfillment of the
Requirements for the Degree of Master of Science

A MOLECULAR DYNAMICS STUDY ON CELLULOSE FIBER REINFORCED NANOCOMPOSITE

By

Shi Li

August 2011

Chair: Youping Chen
Major: Mechanical Engineering

Wood has a hierarchical structure, whose macroscopic properties emerge from their micro- and nanostructural level. In micro- or nano-scale, the mechanical properties of cell wall depend on its molecular interaction. However, due to the complexity of wood cell wall, it is difficult to study the interaction between the components within the cell wall by micro scale experimental sample. Thus, nano-scale simulation is a suitable way for us to study the mechanical properties of wood cell wall.

The aim of this study is to use molecular dynamics (MD) simulation for elucidating the interactions between cellulose and hemicellulose in the secondary cell wall and microfibril angle (MFA) effect on the properties of fiber reinforced composites

The models of cellulose microfibril bundle and hemicellulose matrices were obtained by MD software AMBER. Then topology and force field parameters of these models are transmitted to another MD software LAMMPS. The cellulose microfibril bundle is pulled away from three kinds of hemicellulose matrices. It is found that not only the area but also the shape of hemicellulose chain could affect the interaction between cellulose and hemicellulose. Furthermore, a compression loading has been

applied on the systems with different MFAs. The MFA effect on the mechanical properties and the failure mechanism of the systems has also been studied.

CHAPTER 1
INTRODUCTION

1.1 Wood Components

Wood is composed of cellulose microfibrils (40% - 50%), hemicelluloses (15% - 25%) amorphous lignin (15% - 30%) and extractives. Additionally, structural proteins (1% - 5%) can be found in most plant cell walls. Besides, numerous enzymes are also contained in the plant cell walls. Plant cell walls also contain numerous enzymes, which do not affect the mechanics of structure.

1.1.1 Cellulose

Cellulose is the major chemical component of the cell wall of wood. About 40% - 50% of all plant matter is cellulose. It is a polysaccharide composed of linear chains of D-glucose units. The degree of polymerization can be from several hundred to over ten thousand. These D-glucose units are linked by β-1,4-glycosidic bonds.

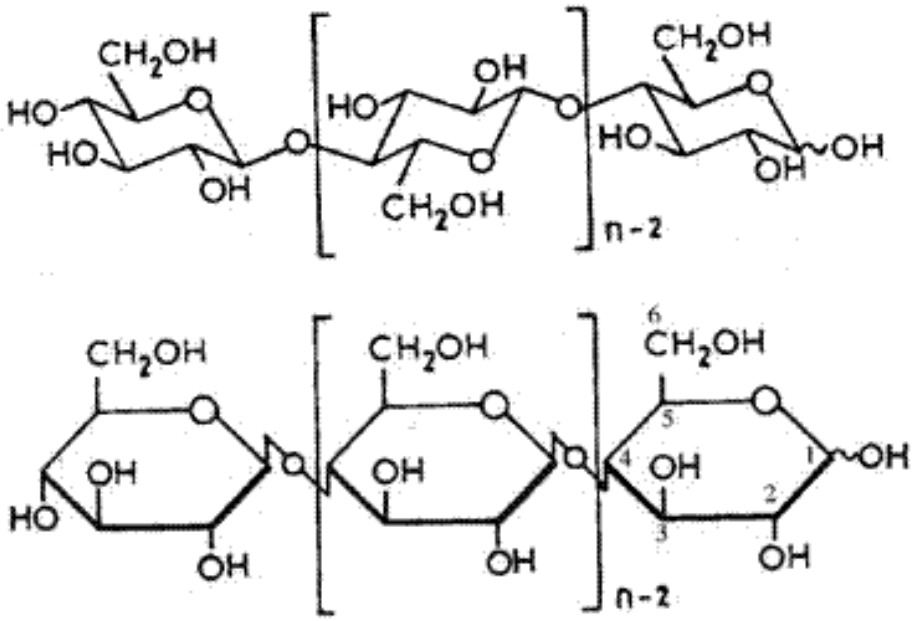

Figure 1-1. The structure of cellulose

The formula of the organic compound of cellulose is $(C_6H_{10}O_5)_n$. Due to the effect of hydroxyl groups at C2, C3, and C6 positions of the D-glucose unit, cellulose has a

strong tendency to form intra- and inter-molecular hydrogen bonds on the linear cellulose chains. The net of hydrogen bonds among the cellulose chains can stiffen the straight chain. Furthermore, the effects of hydrogen bonds can promote aggregation into a crystalline structure.

Native cellulose, which is also called cellulose I, is known to have two distinct crystal phases: the algae Glaucocystis (Iα, triclinic) and the tunicate Halocynthia roretzi (Iβ, monoclinic). The amounts of Iα and Iβ vary depending on the biological samples from different origins. Both of these crystal allomorphs exist in various proportions in different materials. Generally, algae and bacteria are Iα-rich, while higher plant life, like cotton and wood, are Iβ-rich and a small proportion of Iα cellulose. However, only Iβ crystalline allomorph with disordered chains is associated with its crystallite surface in higher plants (Ding and Himmel, 2006). Due to restricted access to water and chemicals, the chemical attack can be expected to occur on the crystalline cellulose surface. Therefore, the Iβ-like form of cellulose is one of the objects this paper concerns.

Due to the activity of the hydroxyl groups, cellulose can provide large amounts of derivatives with useful properties by reacting with various chemicals. The most important commercial materials of cellulosic derivatives are cellulose esters and cellulose ethers.

1.1.2 Hemicellulose

Hemicellulose is a polysaccharide related to cellulose. Generally, it comprises about 20% of the mass of the plant. The hemicellulose can be any of several heteropolymers (matrix polysaccharides). It exists in almost all plant cell walls, usually along the cellulose chains. Even though, the components of cellulose and hemicellulose

are very similar, they have different properties because the structure is quite different. Cellulose is crystalline, so that it is strong and tough. However, hemicellulose is quite flexible with a random and amorphous structure.

Furthermore, cellulose always contains only anhydrous glucose, but hemicellulose can contain varying amounts of sugar monomers, including glucose, xylose, mannose, galactose, rhamnose and arabinose, which can also be found in heteropolyers. In addition, most of the D-pentose sugar and some very small amounts of L-sugars can be found in hemicellulose. Usually, xylose contains mostly hemicellulose in sugar monomers. However, mannosic and galactosic acid are also sometimes found to be comprised of hemicellulose.

In almost all the plant cell walls, hemicelluloses are embedded among cellulose microfibril bundles. They are in the form of chains, which form a network of cross-linked fibers to connect cellulose and pectin. Though cellulose and hemicellulose both exist as a chain in plant cell walls, the length of the chains are quite different. In cellulose, about 10,000 to 15,000 glucose monomers comprise a polymer. But hemicellulose chains consist of only about 200 sugar monomers. Furthermore, some branches of sugar monomers exist on the main chain of hemicellulose, but cellulose is not branched. Xylan, glucuronoxylan, arabinoxylan, glucomannan, and xyloglucan are some common hemicellulose found in plant cell walls.

1.1.3 Lignin

Lignin is another key component of the plant cell walls. Lignin makes up about one-quarter to one-third of the dry mass of the wood. It fills the space between cellulose, hemicellulose and other components of the cell wall and then forms covalent bonds to different polysaccharide. Thus, lignin also connects cellulose, hemicellulose

and pectin. The mechanical strength of the cell wall and even that of the whole plant will be enhanced because of the effect of lignin.

The molecular mass of lignin can be more than 10,000 Da (Da: unified atomic mass unit Dalton). Unlike cellulose and hemicellulose, lignin is so heterogeneous that the primary structure of this kind of biosynthesis could not be defined. The degree of polymerization of lignin is quite difficult to measure. The lignin consists of various kinds of substructures that randomly bind with each other. Due to its structural complexity, there is not a well defined or standard structure for us to build the model. Therefore this study was focused on the fiber reinforced cellulose-hemicellulose system.

1.2 Cell Wall

The plant cell wall is a tough and relatively rigid structure that surrounds the cell. Its thickness can be up to several micrometers. Because of its toughness and rigidity, the plant cell walls provide a defined shape for the cells and protect the cell itself. None of the cell membrane can be comparable in strength to the plant cell wall. The cell wall is the main difference between animal cells and plant cells. The cell wall acts as a filtering mechanism and the major function of the cell wall is to be like a pressure vessel, offering protection against mechanical stress. The composition and properties of the cell wall can be varying depending on the growth conditions and biological samples.

There are up to three kinds of different layers in plant cell walls: primary cell wall, secondary cell wall, and middle lamella.

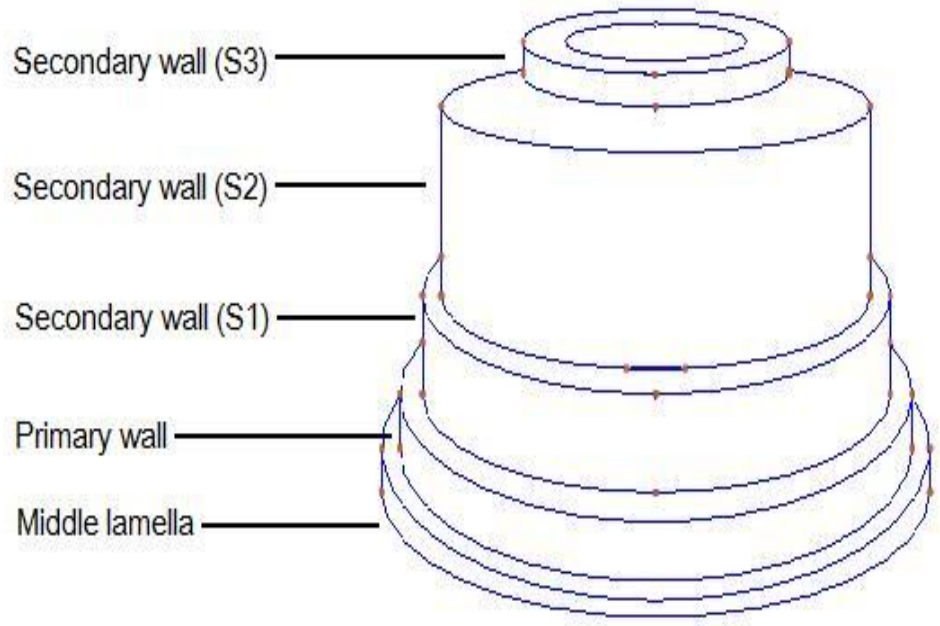

Figure 1-2. Diagrammatic representation of wood secondary cell wall

The cell walls in young cells are thin and flexible, which can allow the cell to grow and expand. The first cell wall of these growing cells is called the primary cell wall. Though it should be flexible enough for growth, it should also be sufficiently strong to protect the cell itself. Several interconnected polysaccharide matrices and a small amount of proteins are contained in the primary cell wall. The matrices consist of cellulose, hemicellulose, and pectins. Xyloglucans and galactoglucomannan are the common components of the hemicellulose chains, while the homogalacturonan and rhamnogalacturonan are often observed to form the pectin matrices.

When the cell is fully grown, the primary cell wall may stay alive, and another new layer may be deposited by the cell. This new layer which is called the secondary cell wall is much thicker than the primary layer. Not all cells contain the secondary cell wall, but the secondary cell wall exists in almost all of the xylem. Though it is can be found anywhere in the plant, the word itself means “wood” and wood is the best known xylem

tissue. Because of the secondary cell wall, wood plants can hold themselves up against gravity. Like primary cell wall, the secondary cell wall also consists of cellulose, hemicellulose and lignin. But the ratios of these components are quite different from that in primary cell wall: instead of xyloglucans, xylan takes more weight and more cellulose exists. Besides, pectins and structural proteins can be absent from the secondary cell wall. Recently, the lignifications of the secondary cell wall was considered to be a key reason for the compressive strength, while the cellulose microfibrils bring the tensile strength to the cell wall, even to the plant. The structure of the secondary cell wall could be imagined as the same as reinforced concrete: cellulose microfibrils act like the reinforcing steel bar, which give the whole structure tensile strength; and the hemicellulose-lignin matrices act as the concrete. Another important interest of the secondary wall is its three distinct layers – S1, S2, and S3. In those three layers, the cellulose microfibrils angles (MFA) are varying, so that the strength of S1, S2, and S3 could be different. Among these three layers, the thickness of the S2 layer is much greater than that of the S1 and S3 layers (Barnett and Bonham, 2004). This means that for the measurement of secondary wood cell wall, the results can be approximated to the mechanical properties of S2 layer.

The middle lamella, which connects the cell walls of adjacent plant cells together, is a layer full of pectins. The outmost layer is very similar to the primary wall, especially when the plant cell has a thick secondary wall. Thus, the compound middle lamella consists of two primary cell walls and middle lamella, and sometimes the secondary wall of two adjacent cells. This layer also provides stability to the plant.

1.3 Software

1.3.1 Gaussian 03

Gaussian is a series of electronic structure packages, which provides state-of-the-art capabilities for predicting all the scientific and modeling features of atoms, molecules, and reactive systems. Without any artificial limitations on calculations, Gaussian can predict the energy, molecular structures, and vibration frequencies of molecular system, by utilizing ab initio, density functional theory, semi-empirical, molecular mechanics, and hybrid methods.

Molecular dynamics is often used as a tool for computational modeling for large scale biomolecular simulation. The length scale for biomolecular simulation is rather small, ranging from 10^{-10} m to 10^{-8} m. Similarly, the time scales of biomaterial motions are from 10^{-15} to 10^{-3} seconds. The length scales implemented in molecular dynamics can fully satisfy the requirements of biomolecular simulation; however, the state-of-art simulation could only do its best to get to 10^{-8} seconds, due to the limit of the efficiency of parallel computers. Although a longer time scale is better, the current MD techniques are sufficient to figure out the internal dynamics within biomolecules.

1.3.2 AMBER

AMBER is a package of programs that can be used to run molecular dynamics simulations, particularly on bio-molecules, such as proteins, nucleic acids, polysaccharides, etc. ”Amber” is also the name of one of the most popular empirical force fields. However, in this software, amber force field is combined with other force fields which can be implemented.

As a molecular dynamics (MD) simulation package, AMBER allows users to build their own model by using some basic residue models and manipulating molecules. Also,

in order to build some unusual molecular, the data generated from experiences or other simulation software can be imported into AMBER. The main program, sander, allows for NMR refinement based on NOE-derived distance restraints, torsion angle restraints, and penalty functions based on chemical shifts and NOESY volumes. The molecular simulation is carried out by sander. Moreover, AMBER includes some post process programs to analyze MD trajectories. A variety of calculations can be computed by AMBER, for example, root mean square deviation (RMSD) from a reference structure, time correlation functions, hydrogen bonding analysis, solvent mediated energy of biomolecules, and so on.

1.3.3 LAMMPS

LAMMPS is an acronym for Large scale Atom Molecular Massively Parallel Simulations. Unlike AMBER which concentrates on bio-molecules, this software can model most systems, like biological material, metal, and coarse grained systems. It contains almost nearly all force fields and boundary conditions. Due to its great efficiency, a simulation with millions or billions of particles can be performed by LAMMPS. Because it is a freely available open source code, users can modify the programs as necessary. And users are encouraged to upload their modifications or updated programs to LAMMPS, which in turn has made LAMMPS a frequently updated. The number of pages in the manual has increased from less than 300 to more than 600, which supports the notion that LAMMPS is one of the most popular MD simulation software.

But LAMMPS cannot do everything. The molecule structure cannot be modeled and sophisticated analyses should not be carried out by the software itself. Furthermore, LAMMPS provides many force field formats, but the parameters of these

force fields should be input by users themselves. Thus, in this thesis, the three kinds of software are used.

1.4 Scope of This Thesis

The goal of this research is to develop a model for the secondary cell wall of wood through computational method. With structural and chemical composition information obtained from existing publications, cellulose microfibrils and hemicellulose matrices, which are the main components in wood cell wall, are obtained by using existing well tested molecular dynamics simulation codes.

Based on the models of wood structural parts, a cellulose fiber reinforced nanocomposite model is developed to identify the mechanical properties and recognize the failure mechanism of it.

Chapter 2 of this thesis is devoted to the details of building the model of cellulose microfibril and hemicellulose chain. The model in Chapter 2 is built by using AMBER, which is a type of software suitable for chemical and biological engineering. To test the mechanical properties of the nanocomposite, in Chapter 3, data obtained from AMBER is transferred to another MD code LAMMPS, which is more professional and efficient. A shear loading is applied on cellulose fiber reinforced nanocomposite to recognize the mechanism of interfacial failure between cellulose microfibrils and hemicellulose matrices in Chapter 4. Chapter 5 is devoted to the mechanical properties of the nanocomposite and the relevance of the microfibril angle (MFA).

CHAPTER 2
CELLULOSE MICROFIBRILS MODELING

2.1 Structure of Cellulose Microfibril

Cellulose is linear chain polymer. It is so straight that no branching or coiling happens on the molecule. The structure of cellulose is a stiff rod-like conformation, which is composed by multiple glucose residues. The hydroxyl groups on the glucose from one chain could form hydrogen bonds with the oxygen molecules on itself or on another neighbor chain. So hydrogen bonds are the major factor to hold the chains of cellulose firmly together. Figure 2-1 shows the conformation of the network of hydrogen bonds.

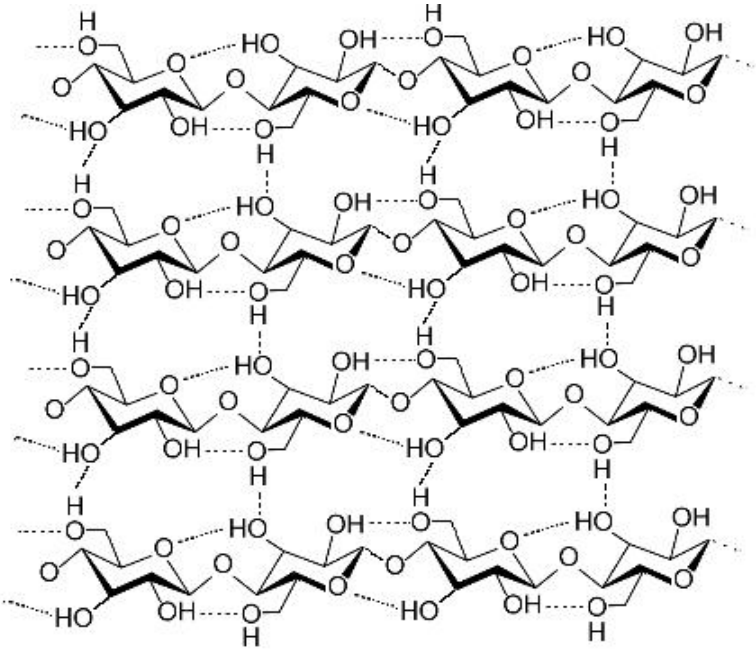

Figure 2-1. The network of cellulose molecules connected by hydrogen bonds

Due to the effect of the network of hydrogen bonds, several chains will aggregate together to form a cellulose elementary fibrils. The elementary fibrils were first observed by X-ray scattering studies, and were named “cellulose microfibrils”. The size of cellulose microfibrils depends on various bio-materials. Ding and Himmel proposed a

model of cellulose microfibril that is composed of 36 chains. This model is derived from direct visualization, so we tried to make a 36-glucan chains model of cellulose microfibril.

Natural cellulose microfibril is known to be divided into two distinct allomorphs, Iα and Iβ. The main difference between these two crystal forms is that Iα has a one-chain triclinic unit cell and Iβ has a two-chain monoclinic unit cell. In solid state, it is observed that the Iα phase could be converted to the Iβ phase. And as mentioned in the previous chapter, the phase cellulose is the predominant component of higher plants, like wood and cotton. Thus, the Iβ phase cellulose is the goal we tried to model.

By using some advanced experimental technology, like X-ray diffraction and NMR spectroscopy, the data of the structure of cellulose Iβ is fully studied by amount of related researches. The unit cell constant for cellulose Iβ is: γ = 96.5°, a = 7.784 Å, b = 8.201 Å, c = 10.380 Å (Nishiyama et al., 2002). The crystal structure of cellulose is shown in Figure 2-2 and Figure 2-3.

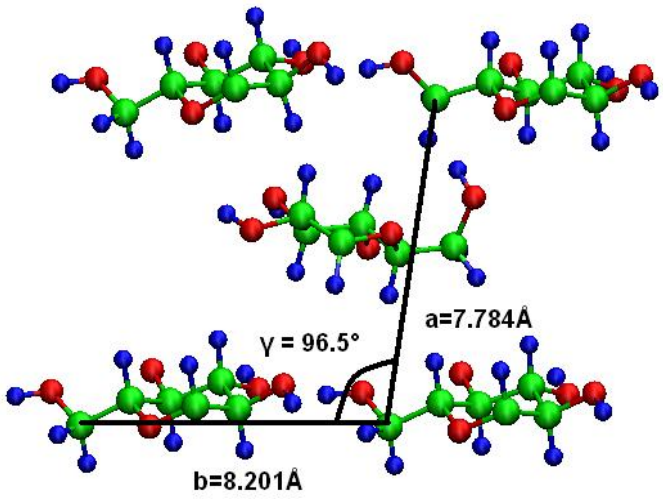

Figure 2-2. View of cellulose Iβ crystal structure along the c-axis

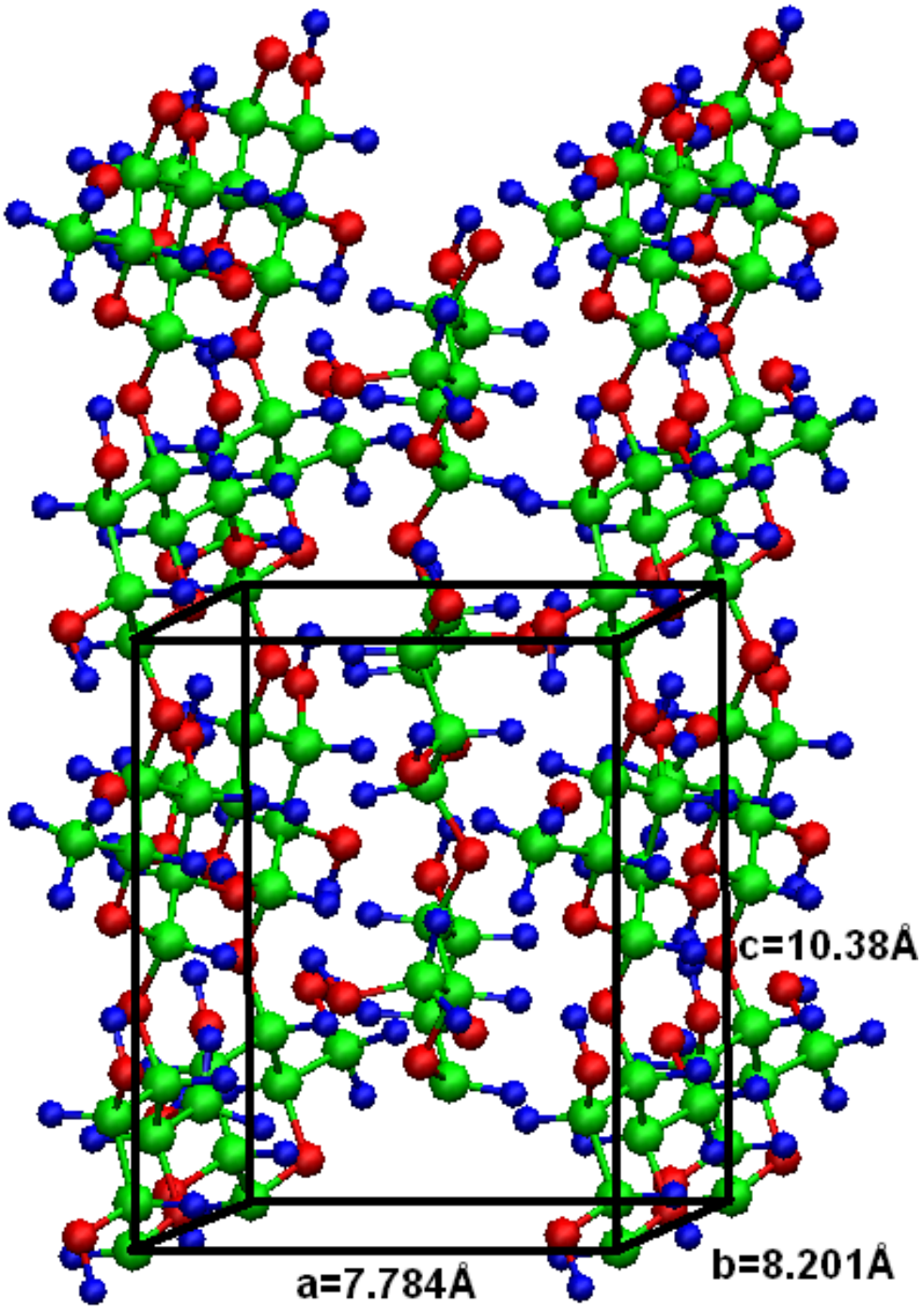

Figure 2-3. View of cellulose Iβ crystal structure obliquely

2.2 Building Cellulose Microfibril in AMBER

2.2.1 Force Field GLYCAM_06

In molecular dynamics simulation, force field is a key factor to determine whether the simulation is reasonable. In AMBER, the choice of force field becomes more important, because it may determine the difficulty in building the model of molecules. Different kinds of force fields will contain different series of basic residues. For example, the one I used for this thesis is call GLYCAM.

GLYCAM comes from the initial letters of Glycosides and glycoproteins with AMBER. This force field is designed to build oligosaccharides and to simulate almost all kinds of carbohydrates. All pertinent force field terms in this force field, have been explicitly specified and so no default or generic parameters are employed. The GLYCAM force field parameters are developed by quantum mechanics. Free energy perturbation and direct deltaG calculations are used to study the structure or sequence of the carbohydrate. Some experimental techniques, such as X-ray diffraction, NMR spectroscopy, and mass spectrometry are employed to combine with the computational methods.

In GLYCAM_06 force field, which is the most updated edition, glucose is one of the standard residues, so the model of cellulose microfibril bundle is based on the glucose residue.

2.2.2 Original Model of Cellulose Microfibril

The unit of cellulose is called β (1->4) linked D-glucose, where β represents β-configuration rotamer, 1 and 4 means the linkage positions are C1 and C4, respectively. Figure 2-4 shows the atomic labeling and the torsion angles parameters of the cellulose chain conformation. The torsion angles are defined by: Φ = O5-C1-O4-C4, Ψ = C1-O4-

C4-C5, Ω = O5-C5-C6-O6, χ2 = C1-C2-O2-H2O, χ3 = C2-C3-O3-H3O, χ6 = C5-C6-O6-H6O.

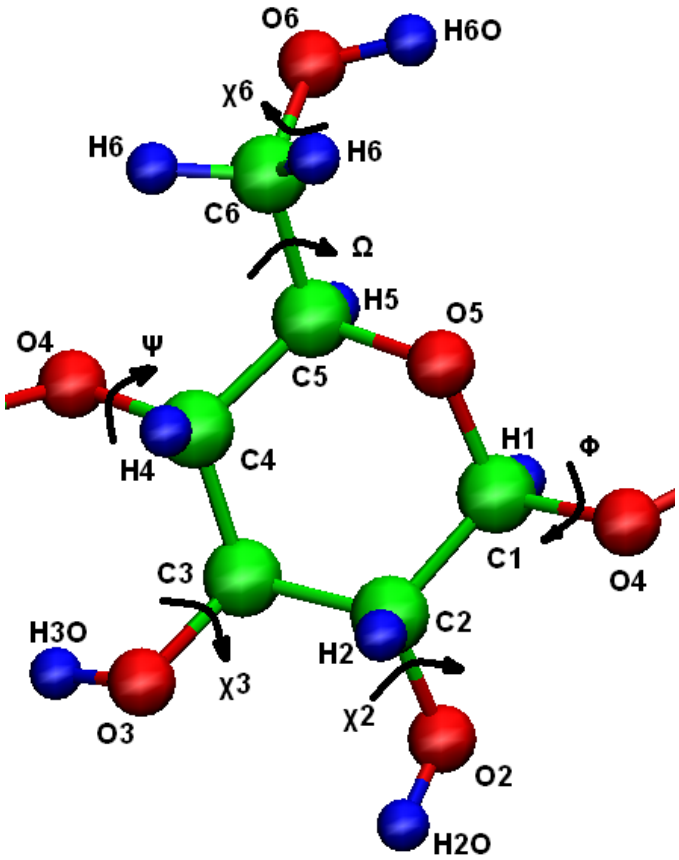

Figure 2-4. Cellulose unit conformation. Atomic labeling and torsion-angle parameters of primary interest are denoted

By employing the package named Leap in AMBER, one chain of D-glucose can be built straight based on the parameters first discovered by Nishiyama et al. (2002). Figure 2-5 shows a part of cellulose chain. Initially, a 21 nm-length chain of cellulose was built. 41 residues are in the chain: the residue on the head of the chain is ROH (-OH), the one at the end of the chain is 0GB, and the other ones in the middle are 4GB. The number “4” in the name of 4GB means the linkage position is C1 and O4. It means that the lack of one hydrogen atom is on those two atoms, so that those two atoms could connect to other residues.

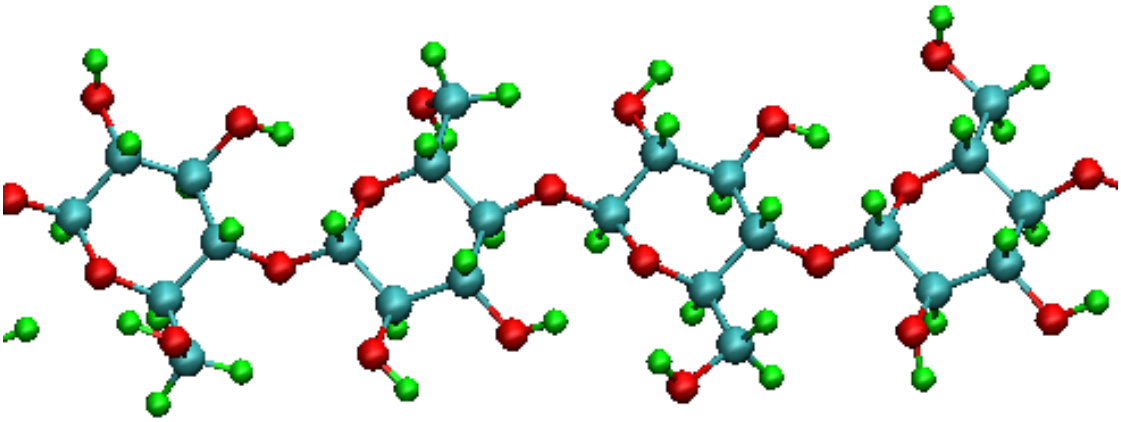

Figure 2-5. Two pairs of cellulose unit (4GB residue) in a cellulose chain

During the modeling, another difficulty is to rotate the chain of cellulose to be parallel to the x-axis. Although it is an original structure, it is difficult to determine the axis of the cellulose chain. When the chain is long enough though, the chain becomes a helix. It means that if all the C1 and C2 atoms are picked out from one chain, the line composed by C1 will not be in the same direction of that composed by C2.

To determine the axis of the cellulose chain, the first and the last GB residues are selected and the branches of the rings that are composed by atoms C6 and O6 are ignored. The ring contains the atoms C1, C2, C3, C4, C5 and O5. After that, the average coordinates of these two rings are calculated as the “center” of both residues. So the line that goes across the two points is considered the axis of the cellulose chain.

The steps for rotation are as follows. Suppose a vector (a, b, c) represents the axis, and our goal is to rotate it to parallel to the x-axis. At first, rotate the vector about the z-axis so that the vector lies in the xz-plane.

Assume θ is the angle. The matrices are rotated by θ about x-axis, y-axis and z-axis which is shown in Eq. 2-1, Eq.2-2, and Eq.2-3, respectively:

$$R_x(\theta)=\begin{bmatrix}1 & 0 & 0 & 0\\ 0 & \cos\theta & -\sin\theta & 0\\ 0 & \sin\theta & \cos\theta & 0\\ 0 & 0 & 0 & 1\end{bmatrix} \quad (2\text{-}1)$$

$$R_y(\theta)=\begin{bmatrix}\cos\theta & 0 & \sin\theta & 0\\ 0 & 1 & 0 & 0\\ -\sin\theta & 0 & \cos\theta & 0\\ 0 & 0 & 0 & 1\end{bmatrix} \quad (2\text{-}2)$$

$$R_z(\theta)=\begin{bmatrix}\cos\theta & -\sin\theta & 0 & 0\\ \sin\theta & \cos\theta & 0 & 0\\ 0 & 0 & 1 & 0\\ 0 & 0 & 0 & 1\end{bmatrix} \quad (2\text{-}3)$$

So the matrix to rotate the vector (a, b, c) about z-axis to xz-plane is Eq. 2-4:

$$R_1=\begin{bmatrix}a/\sqrt{a^2+b^2} & b/\sqrt{a^2+b^2} & 0 & 0\\ -b/\sqrt{a^2+b^2} & a/\sqrt{a^2+b^2} & 0 & 0\\ 0 & 0 & 1 & 0\\ 0 & 0 & 0 & 1\end{bmatrix} \quad (2\text{-}4)$$

Then rotate the new vector R_1*(a, b, c, 1)^T in the xz-plane to the x-axis:

$$R_2=\begin{bmatrix}\sqrt{a^2+b^2}/\sqrt{a^2+b^2+c^2} & 0 & c/\sqrt{a^2+b^2+c^2} & 0\\ 0 & 1 & 0 & 0\\ -c/\sqrt{a^2+b^2+c^2} & 0 & \sqrt{a^2+b^2}/\sqrt{a^2+b^2+c^2} & 0\\ 0 & 0 & 0 & 1\end{bmatrix} \quad (2\text{-}5)$$

Thus, by using rotation matrix, the cellulose chain generated by AMBER can be rotated to x-axis.

It is well known that Iβ phase cellulose has a two-chain monoclinic unit structure. And from synchrotron X-ray and neutron fiber diffraction, the parameters of the unit cell have been determined by Nishiyama et al. (2002). In another one of his papers (Nishiyama et al., 2008), the parameters between two cellulose units are mentioned as Φ = O5-C1-O4-C4 = -98.5°, Ψ = C1-O4-C4-C5 = -142.3°.

Therefore, the whole structure of a 36-chain cellulose microfibril can be obtained by incorporating the same chain structure and arranging it according to the unit cell parameters. The model of our 36-chain cellulose microfibril bundle is shown in Figure 2-6.

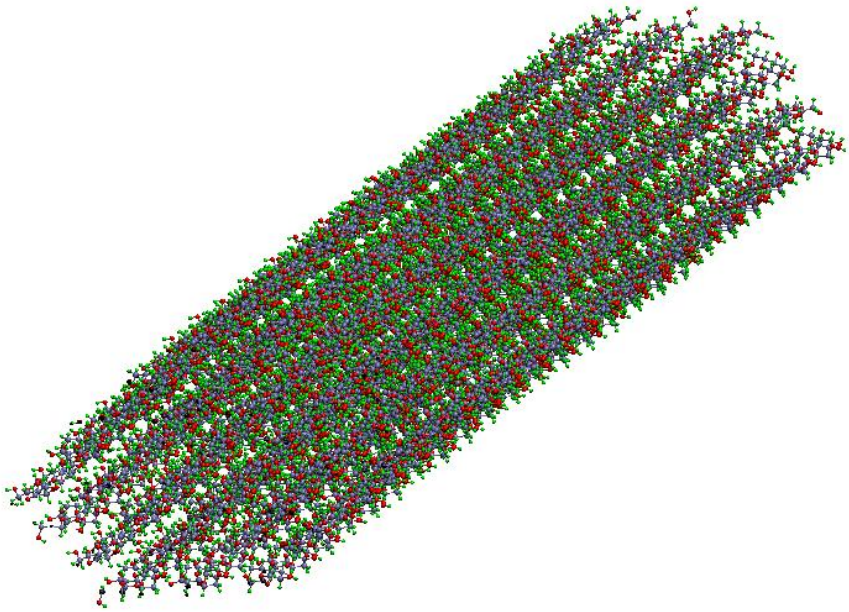

Figure 2-6. The model of cellulose microfibril bundle

CHAPTER 3
HEMICELLULOSE CHAIN MODELING

3.1 Introduction to the Structure of 4-O-methylglucuronoxylans

Hemicellulose can be composed of various sugar monomers, such as glucose, xylose, mannose, and so on. Tracheids and xylem fibers are the main cell types in softwood (gymnosperms) and hardwoods (eudictyledons), respectively, and their walls are predominately secondary. The major non-cellulosic polysaccharides in softwoods are (galacto)-glucomannans, together with small amounts of 4-O-methylglucuronoarabinoxylans. In the cell wall of hard wood, O-acetyl-(4-O-methylglucurono)-xylan, sometimes is also called as acetylated 4-O-methylglucuronoxylan, is the major hemicellulose component. More precisely, the name of this kind of hemicellulose can be written as 4-O-methyl-α-D-glucuronopyranosyl uronic acid xylan. The weight ratio of 4-O-methylglucuronoxylan can be up to 20% of $NaClO_2$-delignified wood. The most representative structure of this polysaccharide is a linear chain of $\beta(1->4)Xyl_p$ units of which a few unevenly distributed residues are substituted at C-2 by 4-O-methylglucuronic acid (Moine and Krausz, 2006).

According to Moine and Krausz's (2007), the ratio of Xylans to methylglucuronic acid ranges from 4:1 to 16:1. The degrees of polymerization of this kind of hemicellulose range from 35 to 230. Then the relative amounts of xylans and 4-O-methyl-α-D-Glycuronic acid were determined by integration of the corresponding anomeric protons, and the ratio of Xylans to methylglucuronic acid was subsequently calculated. Integration results gave an approximate value of 5.9:1, which is in agreement with gas chromatography (GC) analysis. On the basis of experimental data obtained from GC

and NMR analyses, they proposed a theoretical structure model of 4-O-methylglucuronoxylan:

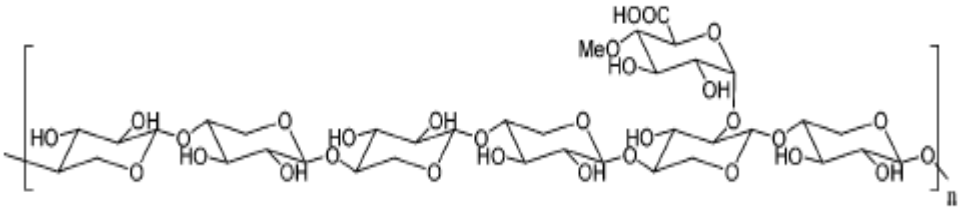

Figure 3-1. A theoretical structural model of 4-O-methylglucuronoxylan

In the figure of unit structure, six (β-1->4)-linked xylopyranosyl residues are arranged linearly to compose the backbone. A 4-O-methylglucuronic acid is substituted at C-2 of one of the six xylan residues, so that the ratio of Xylans to methylglucuronic acid becomes 6:1, very close to the approximate value 5.9:1.

As mentioned above, the main components of 4-O-methylglucuronoxylans are three residues: methyl, glucuronic acid and xylan.

3.2 Build Model with AMBER

It was found that the use of the AMBER force field in conjunction with the GLYCAM parameter set was a very effective method for modeling carbohydrates. However, in GLYCAM_06, which is the most updated force field of GLYCAM series, methyl is not included as one of the group of standard carbohydrate residues. So it is necessary to build a non-standard residue of methyl for our following molecular dynamics simulation with GLYCAM parameter set.

A residue in AMBER should include the following information: topology, atom type, atom charge, bond length, bond angle, torsion angle and dihedral angle. Some of the information can be determined from experimental data and others can be generated by various empirical functions and programs. The topology is always input by users,

because the data comes from experiments. Once the topology is obtained, it was put into Gaussian 03 to get a more reasonable, sometimes more stable electronic structure. Gaussian can also provide the charge distribution of each atom in the molecule. The charge distribution is the most important input when building a non-standard residue, because it can determine the atom type in AMBER. For instance, two atoms may be the same elements, but they may have different orbital hybridization since the charges on the two atoms are not the same, these two atoms belong to two types of atoms, respectively. According to the atom types, bond length and bond angle was calculated automatically in LEaP, which is one important package for building the model in AMBER, by employing the force field parameter set. Torsion angle is not fixed, so this data needs to be obtained by using NMR spectroscopy. At last, dihedral angles ought to be provided by users.

The advantage of Gaussian series of software is that all versions of Gaussian contain every scientific or modeling feature, and none impose an artificial limitation on calculations other than the user's computing resources and patience. In our case, methyl and glucuronic acid are considered as a whole non-standard residue, so Gaussian 03 was used for obtaining the electronic structure and charge distribution of the whole molecule.

Another way to build a hemicellulose model is to take the methyl as a molecule, and then add it to glucuronic acid. Due to lack of information, a single methyl residue was not calculated. First, methyl is so small that we cannot determine its charge distribution when it connects to glucuronic acid and is affected by the electronic cloud of glucuronic acid. Second, even though the charge of methyl is determined, say +1 or -1,

the angles of H-C-H may be different from the realistic situation. Furthermore, even if the accurate structure of a methyl residue was calculated from Gaussian, it is still difficult to connect methyl to glucuronic acid. In order to connect two residues, the data of dihedral angles that is determined by four atoms from these two residues is necessary. Unfortunately, the dihedral angles cannot be readily determined. Thus, the best approach to determine the structure of the branch chain is to calculate the whole methylglucuronic acid, and then a reasonable structure is able to be calculated.

In our case, because of the size of the structure (only 23 atoms are contained in the methylglucuronic acid), a full calculation without any approximation is applied, so that the structure of this non-standard residue can be assumed accurate. After connecting the glucuronic acid residue to the fourth xylan of a backbone, which contains six xylans, a 4-O-glucuronoxylan was obtained.

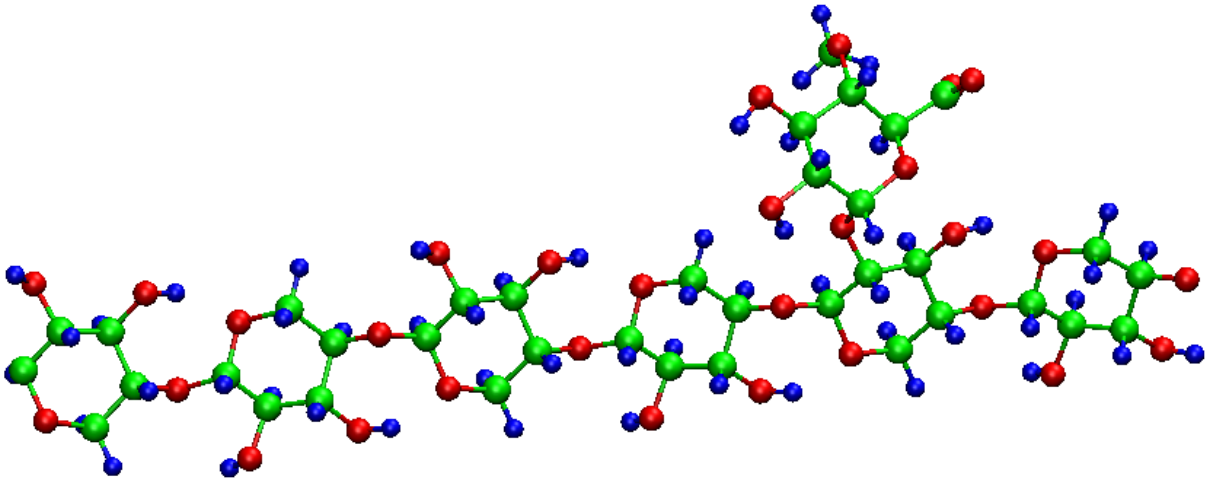

Figure 3-2. Schematic representation of 4-O-methylglucuronoxylan

CHAPTER 4
DATA TRANSFERRING FROM AMBER TO LAMMPS

As I mentioned in the previous chapter, the cellulose microfibril and hemicellulose chains were built in AMBER, and transferred to LAMMPS in order to apply loads on the whole model. There are multiple methods to apply loads in MD simulation: First, is to change the volume and/or shape of the simulation box; another way is to define a group of atoms, and then assign a velocity or force on the group to have a deformation on the whole structure. Moreover, some rigid wall or ball would be used to compress the model.

In these simulations, I employed the first two methods to apply loads, which could be easily performed in LAMMPS. Although AMBER and LAMMPS both are MD software, it is not simple to calculate the mechanical properties of a material in AMBER. There are several reasons why it is difficult to apply loads by using AMBER. First, the periodic box must be introduced if a large-scale molecular dynamics simulation of the model is needed. Even though the concept of the periodic box also exists in AMBER, it is quite different from that in LAMMPS. In LAMMPS, the bonds, angles, dihedrals or anything across the boundaries still have relation with each other, so that multiple periodic boxes could be considered as a whole, whereas only some separated periodic boxes can be simulated in AMBER, since AMBER does not focus on large-scale molecular dynamics simulation. Furthermore, AMBER also allows a group of atoms to be defined and to assign a movement on the group in AMBER, which is so called Steered Molecular Dynamics (SMD). However, no group of atoms happens to be a perfect plane in biomaterial, especially since the model is compressed or stretched. Moreover, it is not possible to employ a rigid wall in AMBER. SMD could apply the force

onto four atoms which can define a plane, but the force could not be applied on the atoms within the plane except the four atoms. That is to say, this plane will not affect the model as a real rigid plane.

In order to apply loads on our biomaterial model made by AMBER, it is necessary to transfer the data or information from AMBER to other MD software, which is LAMMPS.

As two different kinds of software, AMBER and LAMMPS will take different strategies to get the same goal, so all of the settings are not exactly the same. However, the force field and main algorithm should be exactly the same. By using amber2lammps.py, which is provided by LAMMPS website, data can be transferred from AMBER to LAMMPS successfully.

To calculate the same model from AMBER, a proper format of force field should be chosen in LAMMPS. In AMBER, all the force fields are the same format represented as Eq. 4-1:

$$U(R)=\sum_{bonds}K_r(r-r_{eq})^2+\sum_{angles}K_\theta(\theta-\theta_{eq})^2+\sum_{dihedrals}\frac{V_n}{2}(1+\cos[n\phi-\gamma]$$
$$+\sum_{i<j}^{atoms}(\frac{A_{ij}}{R_{ij}^{12}}-\frac{B_{ij}}{R_{ij}^{6}})+\sum_{i<j}^{atoms}\frac{q_iq_j}{\varepsilon R_{ij}}+\sum_{impropers}K_\omega(\omega-\omega_0)^2 \quad (4\text{-}1)$$

The equation above contains the bond style, angle style, dihedral style and pair style.

Bond style set the formula to compute the bond interactions between pairs of atoms. The form of bond style in AMBER is called harmonic, which takes the format as:

$$E=K(r-r_0)^2 \quad (4\text{-}2)$$

Where K is a constant for bond energy and r0 is the equilibrium bond distance.

Angle style helps the users to calculate the angle interactions between triplets of atoms. As the same as the bond style, the angle style is also called harmonic, and the potential could be written as:

$$E = K(\theta - \theta_0)^2 \tag{4-3}$$

Where K is the constant for bond angle energy and θ_0 is the equilibrium value of the angle.

Dihedral style is used for computing the dihedral interactions between quadruplets of atoms. In AMBER, Charmm is the dihedral potential. It can be expressed as:

$$E = K[1 + \cos(n\phi - d)] \tag{4-4}$$

Where K is the dihedral force constant, φ is the equilibrium value of dihedral angle, n is the multiplicity of the function, and d is the phase shift.

Pair style describes the terms for non-bonded pairs of atoms including the electrostatic interactions and van der Waals. So two terms are contained in the expression of pair style lj/cut/coul/cut:

$$E = 4\varepsilon\left[\left(\frac{\sigma}{r}\right)^{12} - \left(\frac{\sigma}{r}\right)^{6}\right] + \frac{Cq_i q_j}{\varepsilon r} \tag{4-5}$$

Where ε is the depth of the potential well, σ is the equilibrium distance where the interactional potential goes to zero, r is the distance between atoms; C is the energy-conversion constant, q_i and q_j are the charges of two atoms, and ε is the dielectric constant. There are two cutoff distances in this non-bonded expression: one is for Lennard-Jones potential and the other one is for the Coulombic pair-wise interaction. The cutoff distances are set for decreasing the computational expense, because the contributions from non-bonded interactions are rather small at long distances. One more

thing should be mentioned is that the Lennard-Jones is different from that in the whole format of the AMBER force field. But these two forms are actually the same.

$$V_{LJ}(r) = \frac{A}{r^{12}} - \frac{B}{r^{6}} \tag{4-6}$$

Where $A = 4\varepsilon\sigma^{12}$ and $B = 4\ \varepsilon\sigma^{6}$. Conversely, $\sigma = (A/B)^{1/6}$ and $\varepsilon = B^2/(4A)$.

The last one is the improper style which describes how to calculate the improper interactions between quadruplets of atoms. However, in our simulation, we do not have to calculate this term, so I do not introduce this expression in this part.

After choosing the right format of force fields, we transfer the coordinate and parameter topology files to a data file, which is used for LAMMPS. Before applying the same algorithm of AMBER, it is necessary to modify some parameters. In AMBER, the dielectric constant is always fixed, and the value is 1. The pair wise interaction, which is also the non-bonded part, is treated differently in various types of force fields. The pair-wise interaction can be divided into three kinds of interactions: 1-2, 1-3 and 1-4. 1-2 interaction is the interaction between a pair of atoms that are connected by a linear bond. 1-3 interaction refers to the interaction between atoms of 1-2 pairs and a bonded third atom. For example, atom A is bonded to atom B, and atom B is bonded to atom C, then the 1-3 interaction here is the interaction between atom A and C. 1-4 interaction is the one that between pairs connected by a set of two bonds. For instance, atom A is bonded to atom B, and atom B is bonded to atom C, and atom C is bonded to atom D, then 1-4 interaction refers to the interaction between atom A and D. In order to calculate the weighted pair wise interactions, the list of bonds, angles or dihedrals will not define the 1-2, 1-3, and 1-4 interactions. And in different force fields, these three interactions have different weights. In AMBER force field, the three coefficients in front of the three

parts are set to 0.0, 0.0, 0.5 for Lennard-Jones interactions (Van der Waals) and to 0.0, 0.0, 0.8333 for Coulombic interactions (electrostatic interactions).

What is different from other kinds of material is that the SHAKE algorithm is applied on the biomaterial. By applying the SHAKE algorithm, the specified bonds and angles are reset to their equilibrium lengths or angular values on each time step. This is done by applying an additional constraint force so that the new positions preserve the desired atom separations. The equations for the additional force are solved via an iterative method that typically converges to an accurate solution in a few iterations.

In AMBER, bond lengths and angles involving all hydrogen atoms are constrained with the SHAKE algorithm, so that the model could be stable. In the molecular simulation by using LAMMPS, the model obtained by AMBER was used as the initial model with SHAKE applied for bonds involving hydrogen atoms and a time step of 2 femtosecond (fs).

In order to figure out whether the data is transferred from AMBER to LAMMPS successfully, I compared each energy term in the initial time step of AMBER against that of LAMMPS. The comparison of each energy term is shown in Table 4-1:

Table 4-1. Static energy analysis of a representative structure of the cellulose microfibril, using both AMBER11 and LAMMPS

	AMBER (kcal/mol)	LAMMPS (kcal/mol)
bond energy	4624.9973	4624.9973
Angle energy	17319.9779	17319.9779
Dihedral energy	26877.7002	26877.7002
Total van der Waals	-46506.7695	-46506.7696
Total electrostatic	261864.3796	261873.4431
Total energy	264180.2856	264189.3489

Since the same force field was chosen for these two kinds of software, the bond energy, angle energy and dihedral energy are exactly the same. There are very small

differences in computing the van der Waals and electrostatic energy, which lead to the difference in the total energy. But it is acceptable for the result, because the internal architecture of the AMBER code is different from that of LAMMPS and these numbers are the sum of several hundred individual interactions. Therefore, the table above shows that AMBER and LAMMPS can calculate nearly identical energies by giving the same original structure, force field, and algorithm.

It is also quite important to check whether the model works after transferring data from AMBER to LAMMPS. In MD simulation, the stability of the model is the most important point to check whether the model works, because the stability of the model determined whether the result converges successfully. If the result diverges as the program runs, the numbers in the model will blow up and never reach a solution. So the cellulose microfibril is relaxed under NPT ensemble for 150,000 time steps, and each time step is 2 fs. In this model, the relaxation time lasted 0.3 ns. To check whether a model is stable, the temperature and the total energy of the model are checked.

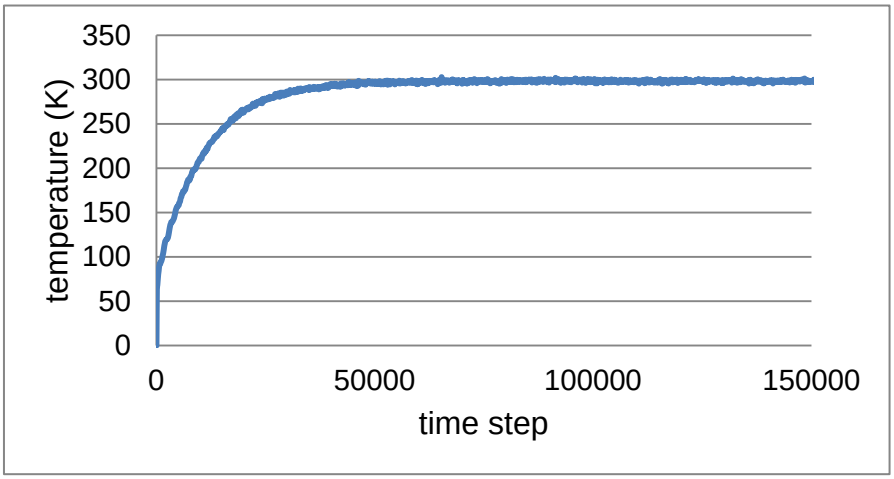

Figure 4-1. Temperature variation during a 150,000-timestep relaxation

From Figure 4-1, the temperature is very stable after about 50,000 time steps around 300K, which is room temperature. At the beginning, the temperature should be

zero, because the initial structure is totally static. Not only is the temperature stable, but the curve of total energy is also correspondingly flat after 50,000 time steps.

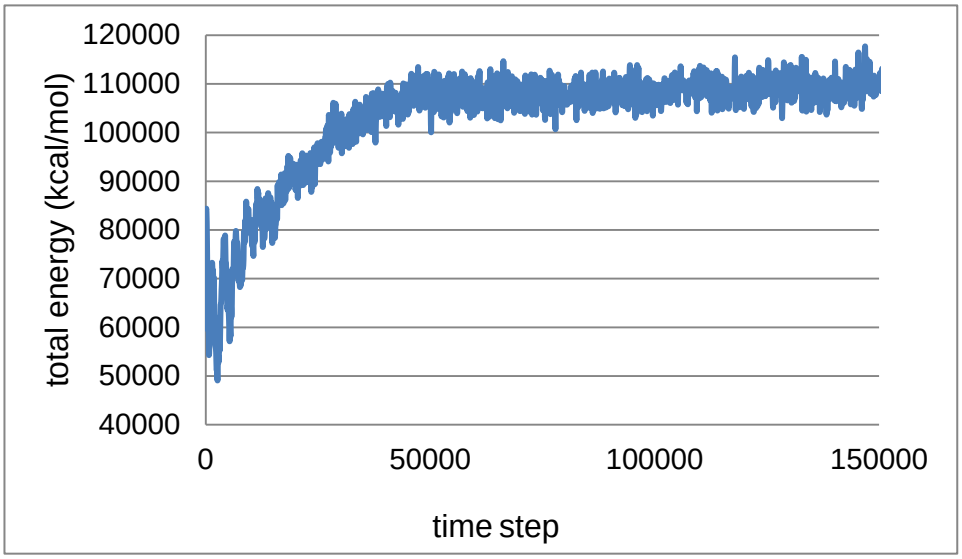

Figure 4-2. Total energy variation during a 150,000-timestep relaxation

CHAPTER 5
INTERFACIAL INTERACTIONS

As mentioned before, the hemicellulose-lignin matrices act as the concrete. The reinforcement of hemicellulose could enhance the stiffness of the wood cell wall. The polymer properties could lead to the mechanism of cell wall deformation. However, it is difficult to analyze the polymer properties by experiment in nano-scale. Thus, the understanding of the interface between cellulose microfibrils and hemicellulose chains is very important and could be used to optimize the properties of the whole structure. It is believed that the interface plays an important role to improve the stiffness and strength of the polymer material. So the interfacial interaction is the focus when the upper cellulose microfibril is pulled away from hemicelluloses matrices in the axial direction.

In traditional polymer matrix composites, the push-out and pull-out test are the particular ways to evaluate the shear strength of the interface. A critical axial load would be applied to debond the fiber from the surrounding polymer. The critical axial load can be used to estimate the shear stress. However, the shear stress in simulation can be much more compliant. Three models were proposed to simulate the effect of the structure of hemicellulose chains. In the simulation, similar to the experiment, the upper cellulose microfibril was applied on an axial load, and the lower microfibril was fixed. The hemicellulose chains, including the ordered long hemicellulose chains and the randomly short ones, were set free.

5.1 Molecular Structure of the Cellulose-Hemicellulose System

Due to the shapes of the ordered hemicellulose chains, I named these three models: u-model, z-model and r-model. All of the three models contain some random hemicellulose chains. Besides that, the cellulose microfibrils are surrounded by only

random hemicellulose chains in the r-model. The topologies of these three models are shown in Figure 5-1, Figure 5-2, and Figure 5-3.

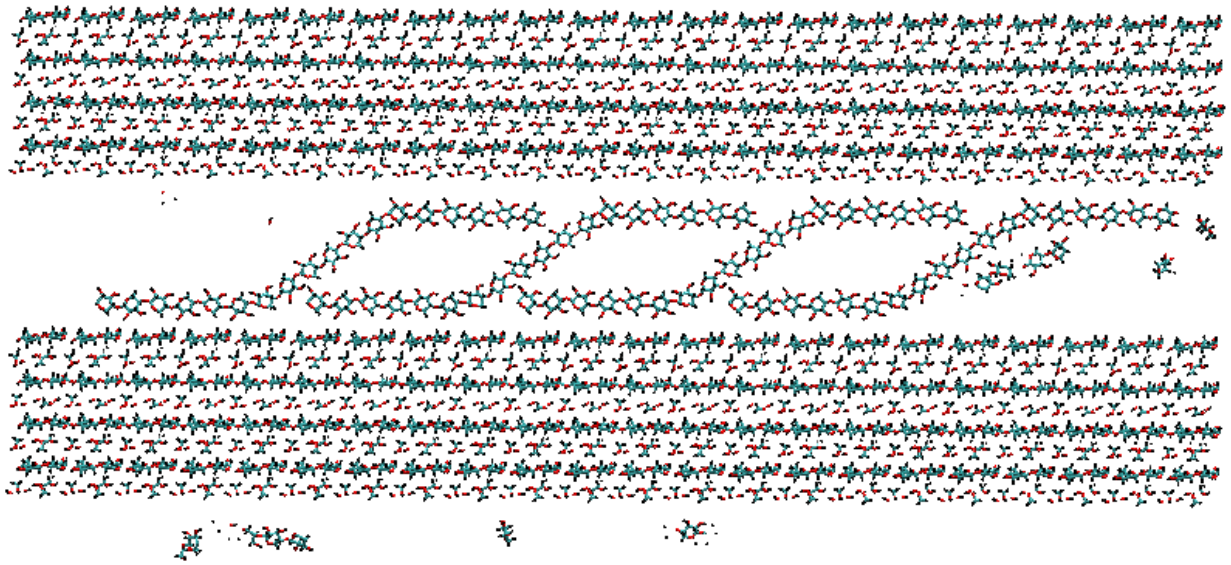

Figure 5-1. A cross-sectional side view of a one layer z-model

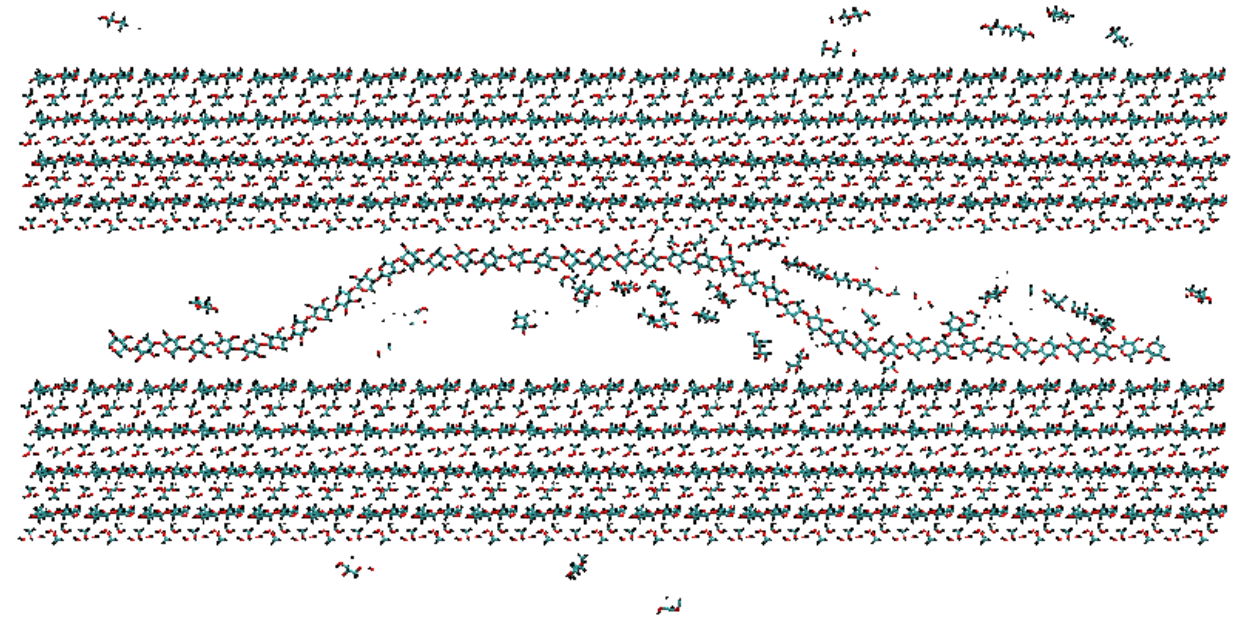

Figure 5-2. A cross-sectional side view of a one layer u-model

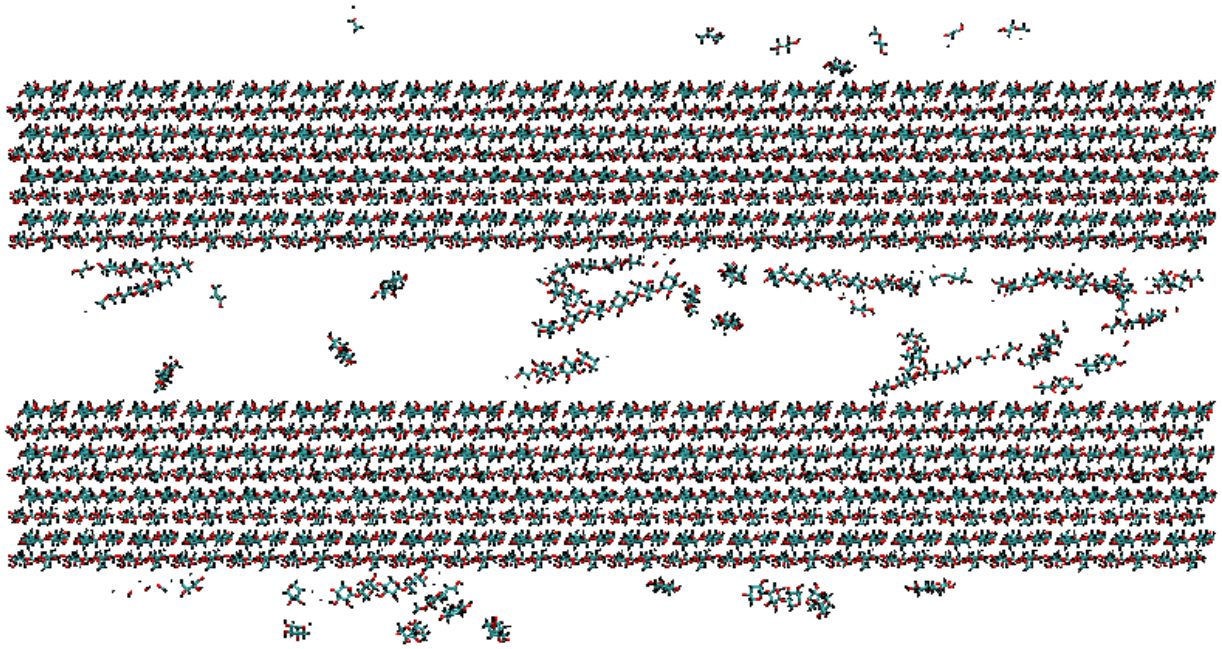

Figure 5-3. A cross-sectional side view of a one layer r-model

The dimensions of each of the three systems are 23.474 × 12.6 × 9.0 nm. All three of these models contain 89112 atoms, and the cellulose microfibrils are all the same. The bonds on the edges of cellulose microfibrils can go across the box boundary, and the models are placed in a three-dimensional periodic box, so the fiber is infinite long. Although the shapes of hemicellulose chains are different, the amounts of the hemicellulose are the same.

The entire pulling process was carried out by MD simulation. An x-axial load was applied on the upper cellulose microfibril to pull it away from the hemicellulose chains around it. The whole simulation contains over 200,000 MD time steps of 2 fs, depending the load variation. The applied force was increased gradually during the whole loading time.

5.2 Relaxation of the Whole System

Actually, the hemicellulose matrices are not connected to the microfibrils in the initial structures. Therefore, several stages of relaxation were taken for the full connection between cellulose microfibrils and hemicellulose matrices.

In the first stage of relaxation, the system was placed under NVE ensemble. All the polymers were set as rigid bodies except the random hemicellulose chains. The cellulose microfibrils and ordered hemicellulose chains are treated as rigid bodies because the rigid bodies can be moved to a lower total potential energy during this 10,000 MD time steps relaxation. This prevents any extremely high interaction in the system.

In the second stage, cellulose microfibrils were still set as rigid bodies, but the hemicellulose matrices were released. Therefore, the hemicellulose matrices can change freely to a less constrained shape and place for MD simulation. The aim of this relaxation is to fully connect the hemicellulose matrices to the cellulose microfibril bundles, due to the electrostatic interactions and Van der Waals forces. This stage also took 10,000 MD time steps.

At last, the whole system was released, so that the cellulose microfibrils and hemicellulose matrices could fully contact with each other. The ensemble for this stage of relaxation is NVT, so that the temperature of the system could be improved to around 300K, which is approximately room temperature. A 100,000 MD time steps are necessary in this stage to fully relax the whole system.

As mentioned in the previous chapter, checking the stability of temperature and total energy during the simulation is one of the most important methods to determine whether a system is stable enough. The figures below show the temperature and total

energy of the z-model during the third stage of relaxation. Similarly, the performance of the u-model and r-model are almost the same.

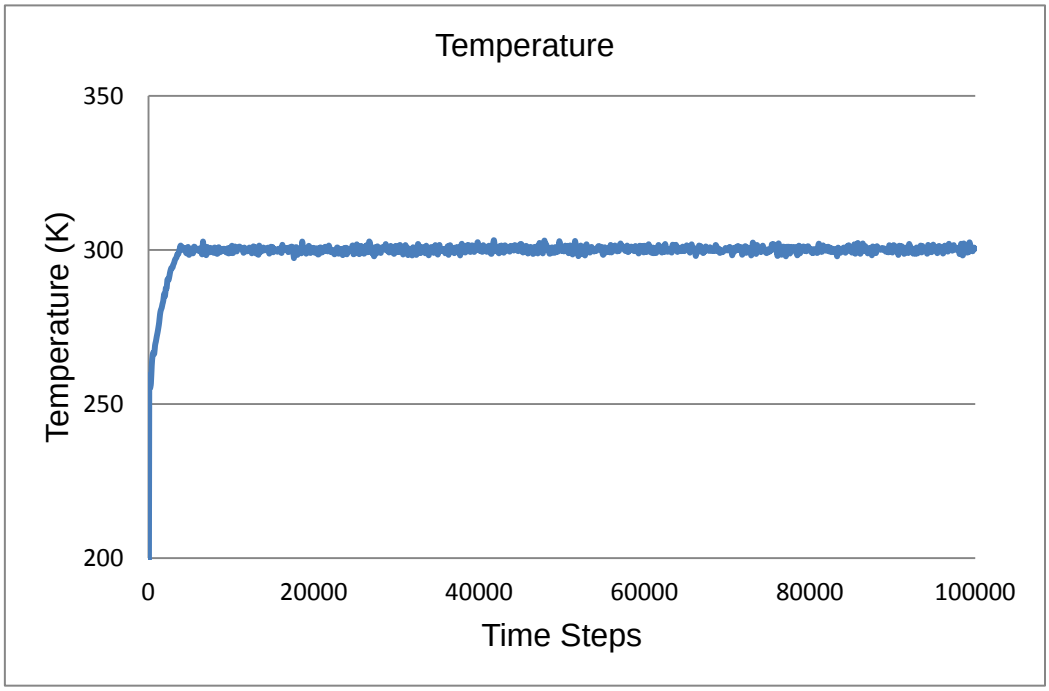

Figure 5-4. Temperature variation during a 100,000 time step relaxation

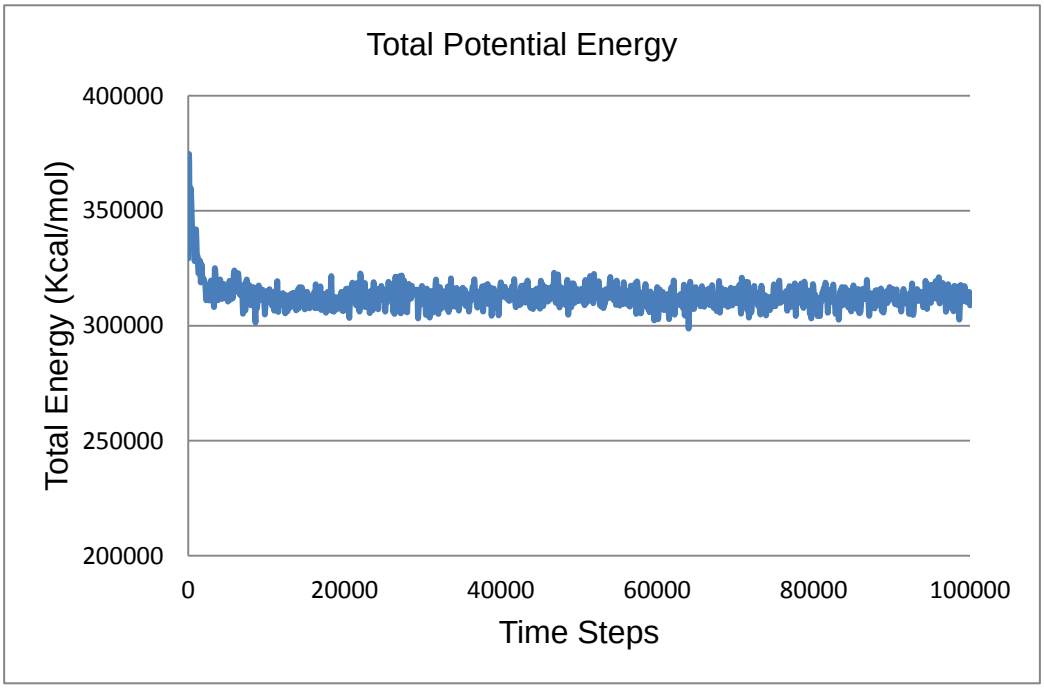

Figure 5-5. Total potential energy variation during the 100,000 time step relaxation

5.3 Applying Velocity with Water Effect

In MD simulation, there are two methods of applying loads to model the pull-out process: one is to set velocities on groups of atoms and the other one is to give an additional push to atoms in the simulation.

At first, velocities were assigned on the upper cellulose microfibril. The systems in this part of simulation were also put into a box full of water. The molecule of water chosen was TIP3P, which is one of the most widely used model for chemical computation. The force of water and hemicellulose matrices on the moving cellulose microfibril was measured. Although the cellulose microfibril moved away from the hemicellulose matrices with various velocities, the force is not realistic.

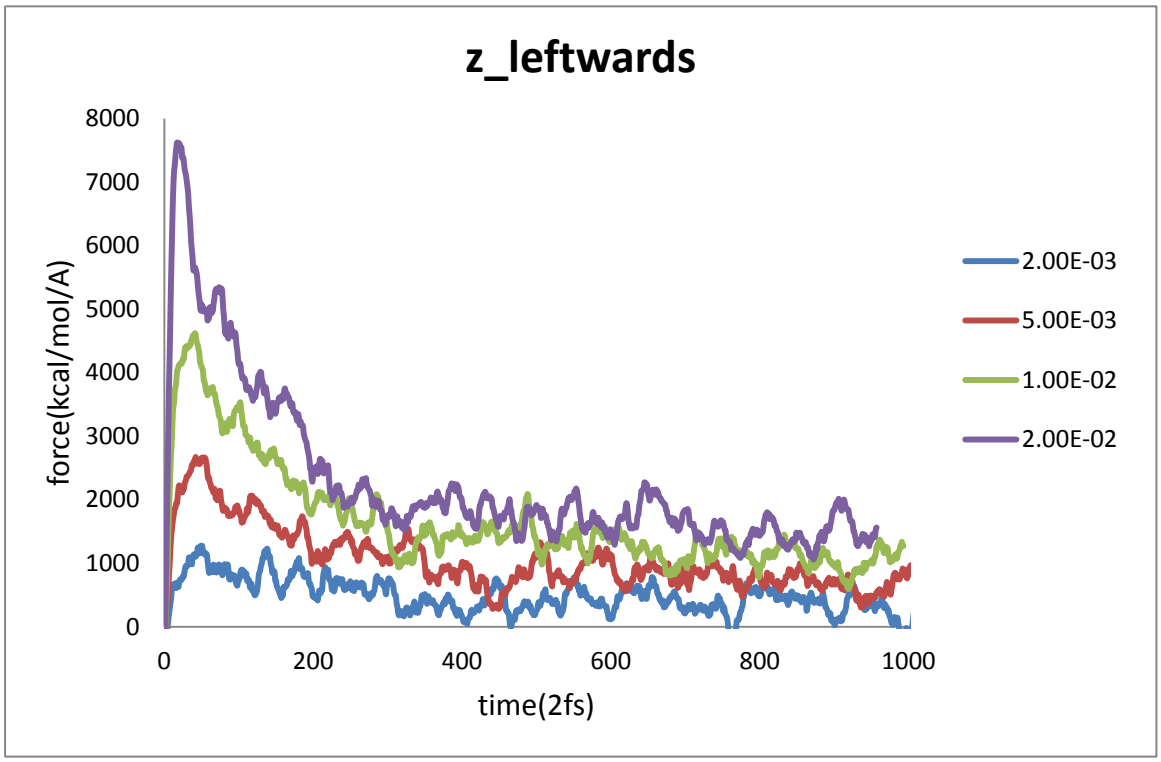

Figure 5-6. Force versus time curves of the z-model upper cellulose microfibril

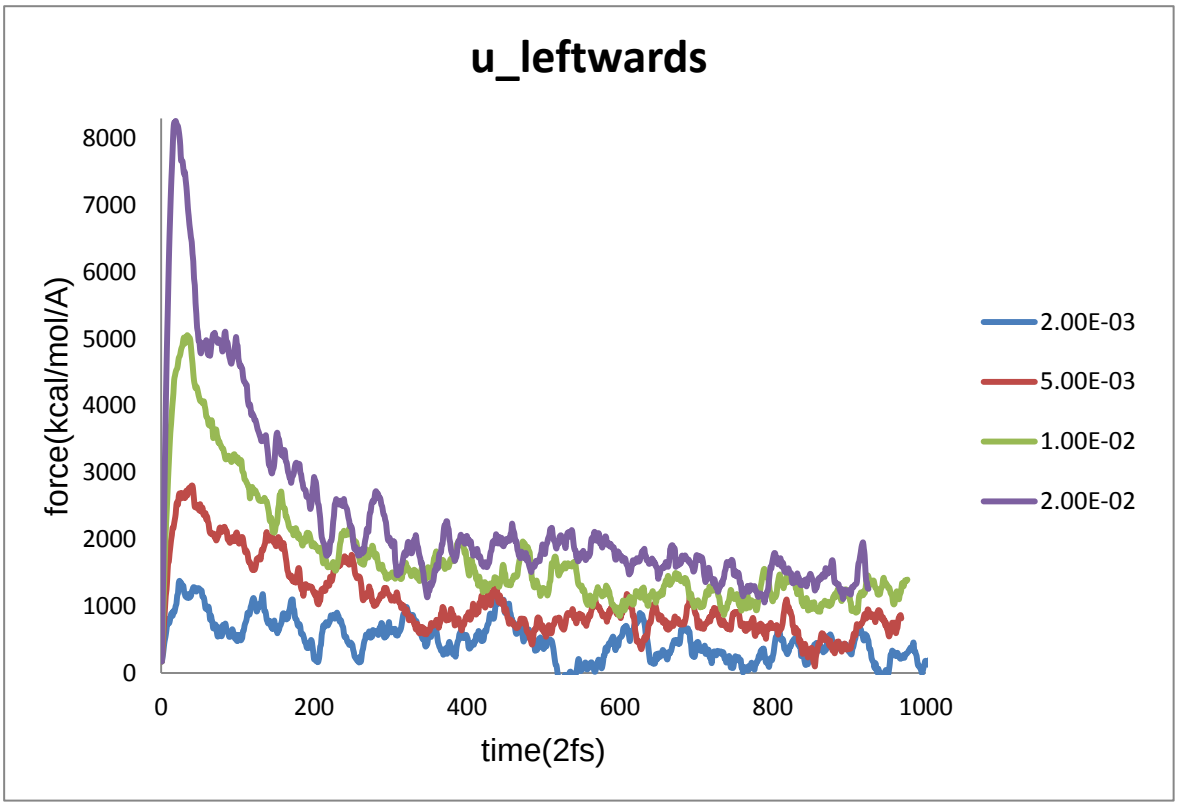

Figure 5-7. Force versus time curves of the u-model upper cellulose microfibril

In Figure 5-6 and Figure 5-7, different curves represent different loading velocities of the upper cellulose microfibril. It seems that the property of the interface depends on the loading rate. The bigger the velocity assigned on the fiber, the larger the force between fiber and hemicellulose matrices is. However, the different models have almost the same curves under the same loading rate. The results may not be reasonable because: a) applying loads on fibers by assigning velocity is not accurate in this case and b) TIP3P water model is not suitable for the simulation of the mechanical properties of this material.

5.4 Applying Incremental Increasing Loads with Water Effect

The other way to apply loads on the same system was then attempted. The advantage of applying increasing force on the material is that both the elastic and plastic deformation stage can be observed, while the elastic deformation stage is very

short if the velocity is assigned on the group of atoms. On each time step of MD simulation, an atom will be affected by the atoms around it. If the velocity of the atom is too small, the atom might be pulled back. If the velocity is big enough to outweigh the effects of atoms around it, a “plastic deformation” will take place. That is why the elastic deformation stages are so short in Figure 5-6 and Figure 5-7.

Assuming the TIP3P water model works fine in MD simulation, the same increasing forces were applied on the fibers of the three systems. As in the previous velocity loading case, the forces of water and hemicellulose matrices on the moving cellulose microfibrils were measured. The force versus displacement curves of the three models are shown in Figure 5-8,

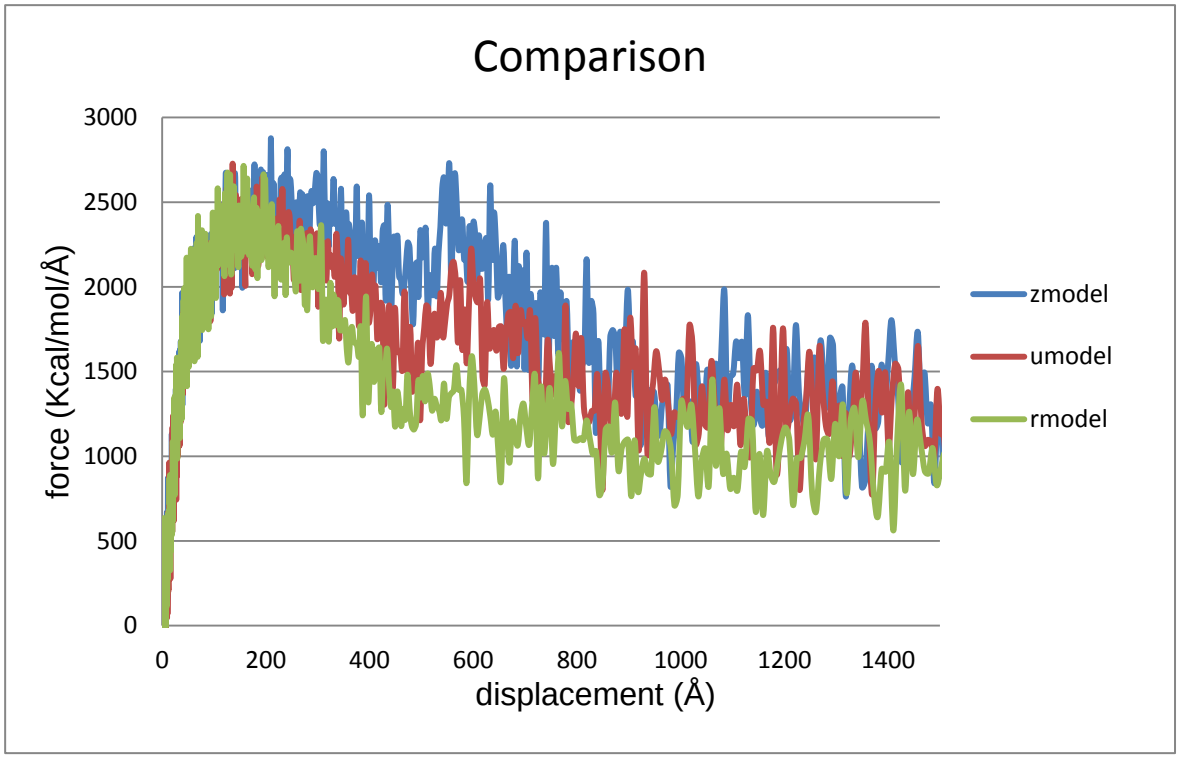

Figure 5-8. Force versus time curves of the upper cellulose microfibrils with water

Although the amounts of hemicellulose matrices are exactly the same in those three models, the contact areas between cellulose microfibrils and hemicellulose

matrices are quite different because of the structures. The connection between two cellulose microfibrils in the r-model is smaller than the other two, so the resulting curve should be the lowest. From the figure above, the maximum force of these three models are almost the same, however, the energies for failure could be depicted by the areas under the force-displacement curves are different. Assuming the contact areas between fibers and hemicellulose matrices of z-model, u-model and r-model are Az, Au, and Ar, respectively. Since Az is the largest and Ar is the smallest, the sequence of energies for material failure is the same as that of the contact area. However, the peaks of these three curves are almost the same, which means there is rarely a difference between the largest forces to pull the fiber out from three different polymer environments. This result is reasonable, but it includes the effects of water.

5.5 Applying Incremental Increasing Loads without Water Effect

The three systems are changed in this part. All the molecules of water were deleted from the periodic boxes. In our simulation, the system of unit is called *real*, so the unit of distance is Å, and the unit of force is Kcal/(mol*Å). After the 120,000 time steps relaxation, 0.01 Kcal/(mol*Å) would be applied on each atom of the upper fiber for every 5,000 time steps. Because the total number of the atoms of one fiber is 33,264, the increasing force applied on the upper cellulose microfibril for every 5,000 time steps is $2.3*10^{-11}$ N. And the force is increased 10 times, so the whole pull process is a 50,000 MD simulation time steps. The force-displacement curves of three models are shown in Figure 5-9,

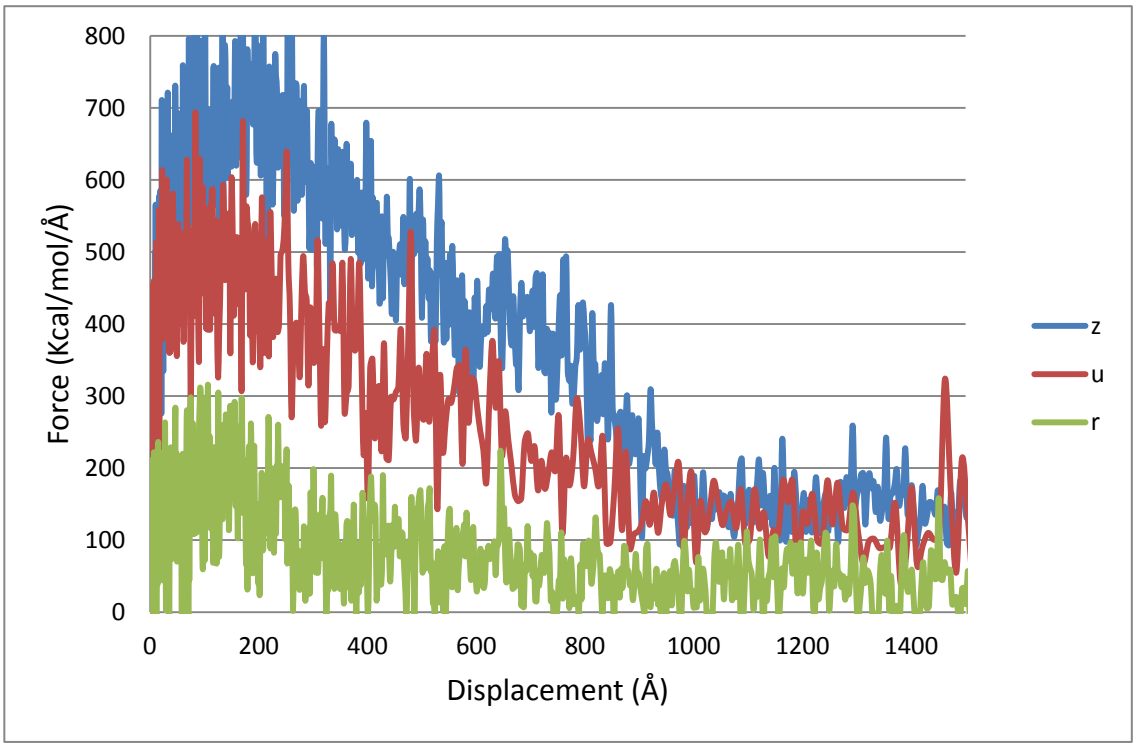

Figure 5-9. Force versus displacement curves of the upper cellulose microfibrils without water

From the atomic trajectory of the systems, the hemicellulose matrix is released when the force-displacement curve began to drop.

It is obvious that the curves of three models are quite different. Two possible reasons for this could be: a) the contact areas between cellulose microfibril and hemicellulose matrices of three systems are different, b) the shapes of the hemicellulose matrices in three models are different.

5.6 Molecular Simulation Applying Loads in Two opposite Directions on Z-Model

Two forces in two opposite directions were applied on the z-model to figure out the effect of the shape of the ordered hemicellulose matrices. Applying loads on the same model can ensure that the contact areas of the interface are always the same. Furthermore, two opposite forces, which are along the positive x-axial and the negative x-axial direction respectively, could lead to an equivalent state of changing the shape of

hemicellulose matrices. That means the structure of the interface was rotated by 180° about y-axis. As in the previous section, the same increasing force is applied on the upper cellulose microfibril bundles.

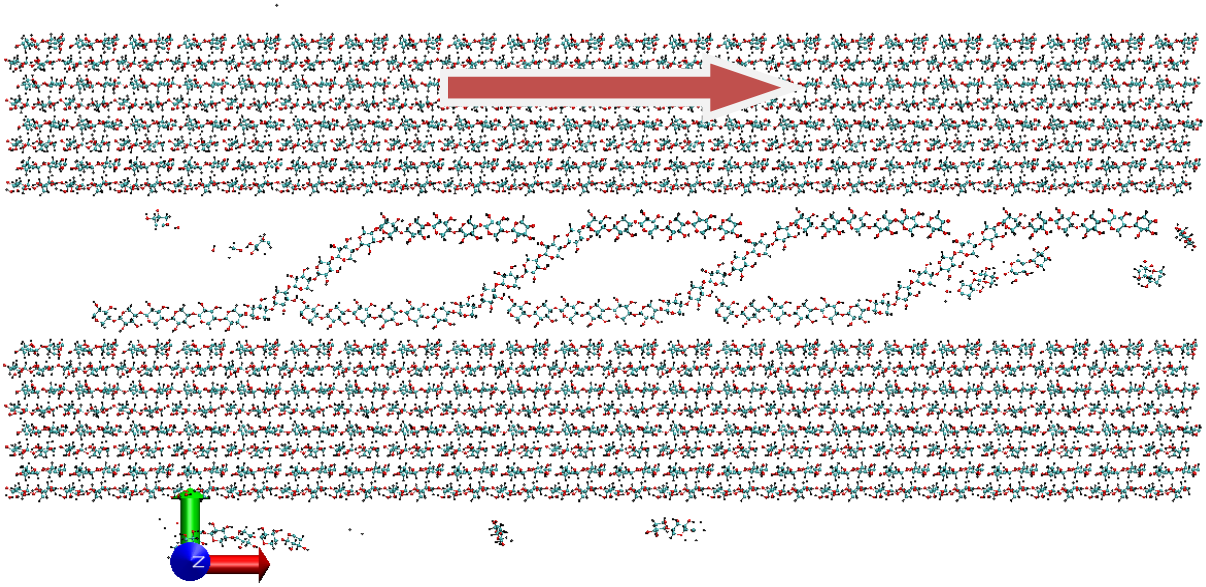

Figure 5-10. Force diagram of the positive x-axial loading

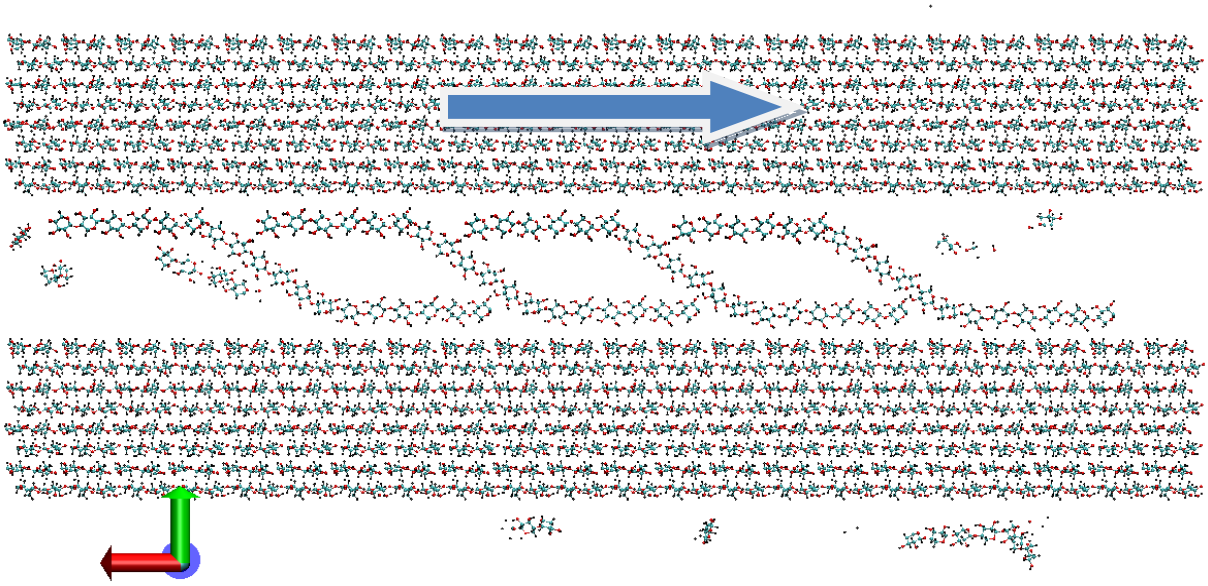

Figure 5-11. Force diagram of the negative x-axial loading

Figure 5-10 and Figure 5-11 show how the forces are applied. After applying the same loading forces on both of the models, the force-displacement curves were generated, which are shown in Figure 5-12 and Figure 5-13.

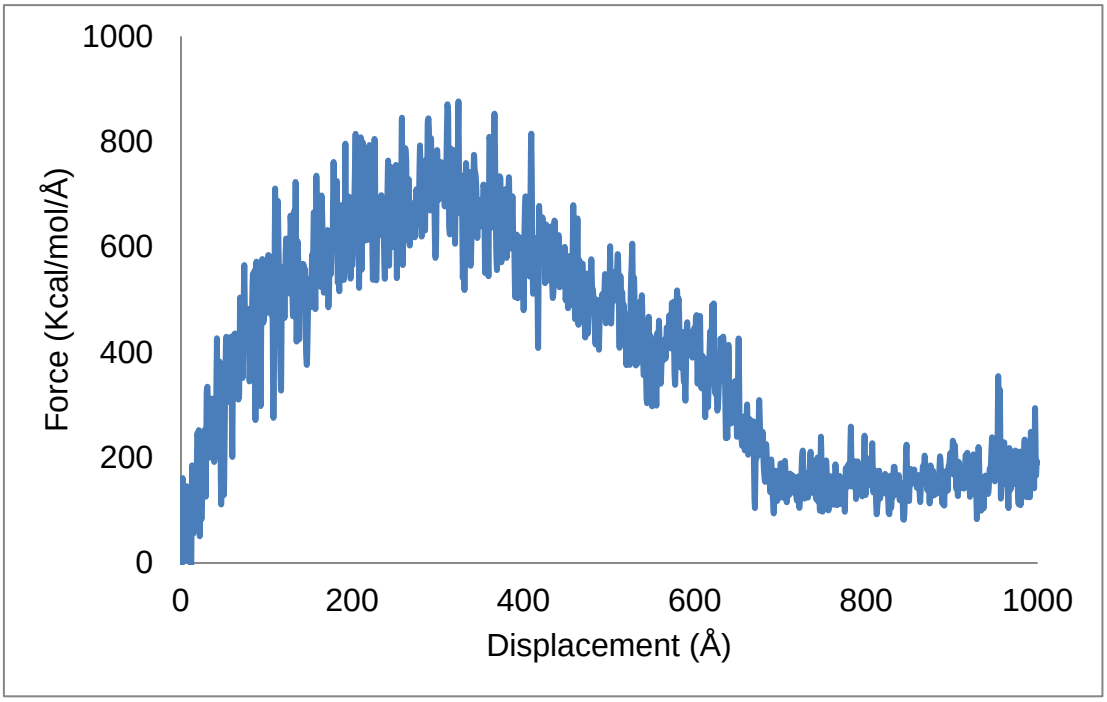

Figure 5-12. Force-displacement curve of the positive x-axial loading simulation

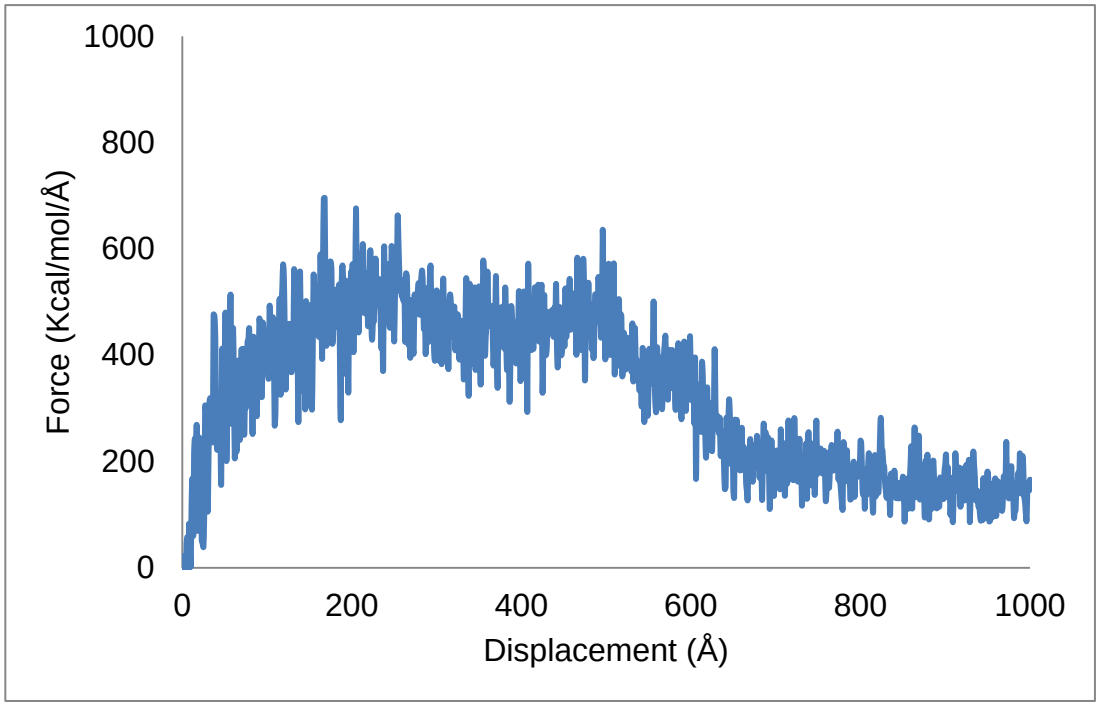

Figure 5-13. Force-displacement curve of the negative x-axial loading simulation

It is observed that these two curves are almost the same except the peak area. When the force is applied along the positive x-direction, the interface allows much more shear force. Since the contact area of these two systems is the same, the shape or the structure should be the main factor to cause the difference. Thus, the trajectories of the atomic structure of the systems were observed.

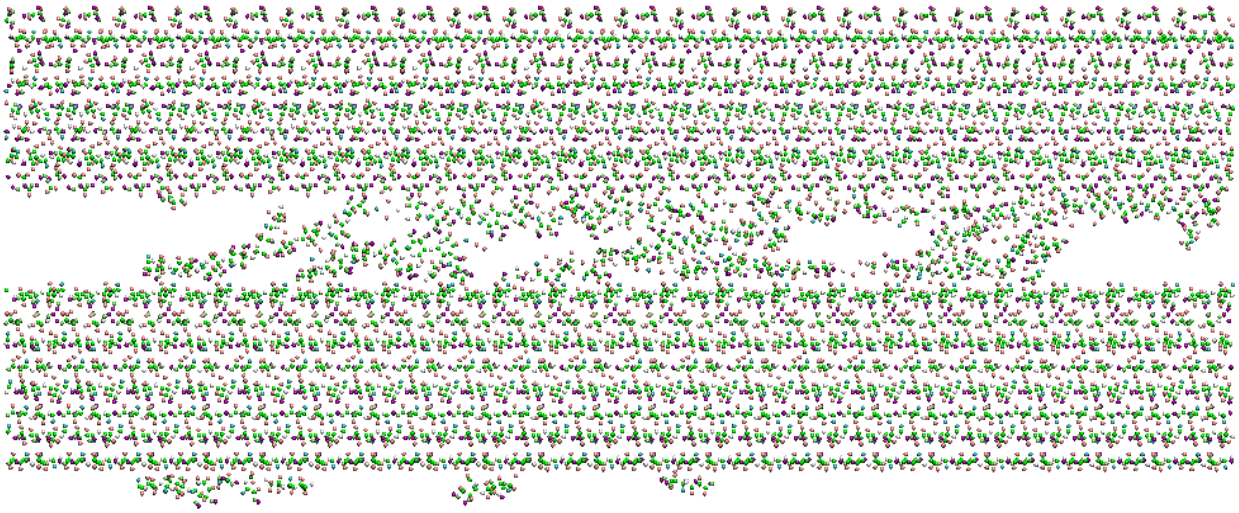

Figure 5-14. A cross-sectional view of a one layer z-model relaxed structure

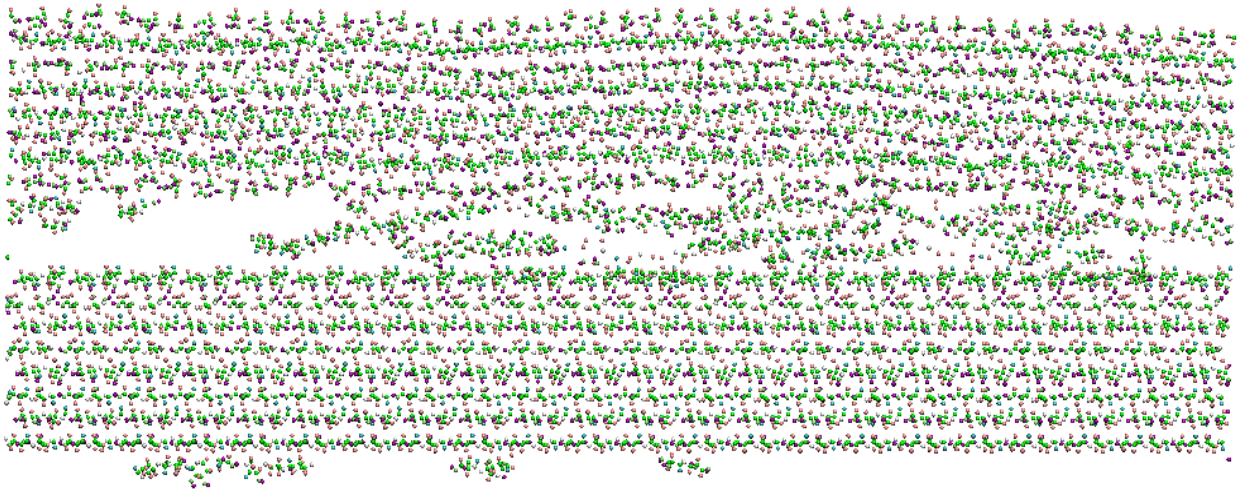

Figure 5-15. A cross-sectional view of one layer structure when the cellulose microfibril is released from hemicellulose matrices under the positive x-axial loading

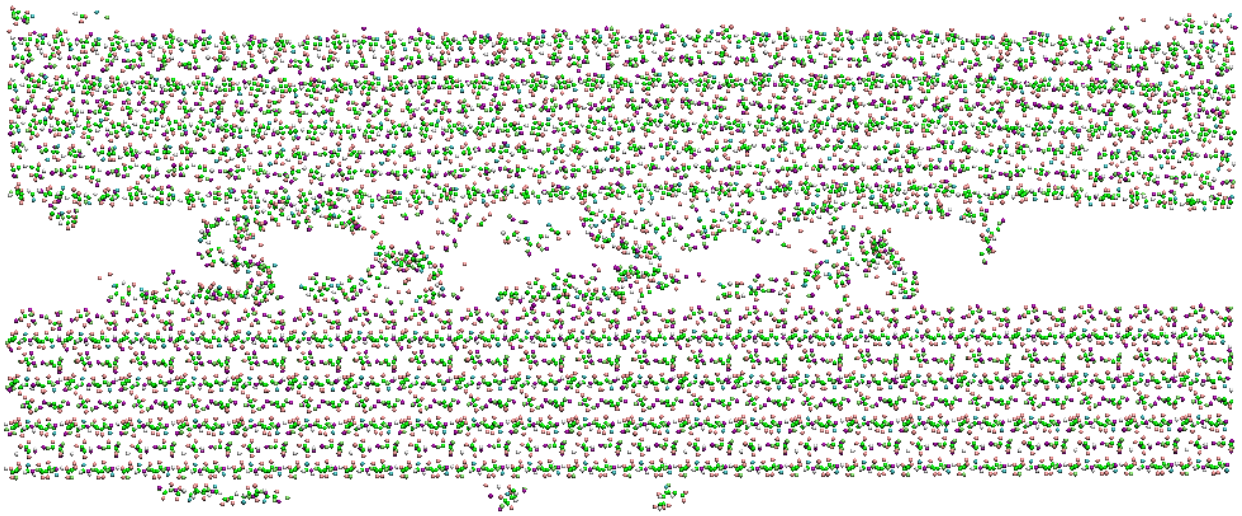

Figure 5-16. A cross-sectional view of one layer structure when the cellulose microfibril is released from hemicellulose matrices under the negative x-axial loading

There are two kinds of groups in one single hemicellulose chain: the upper and lower parts which contact with the cellulose microfibril, and the middle part, which just connect the upper and lower parts. After observing the movement of the atomic structure of these two systems, the adhesive parts of hemicellulose matrices in both systems is released from the cellulose microfibrils when the displacement is about 50 nm showing in Figure 5-15 and Figure 5-16. When the displacement of cellulose microfibril is between 20 nm and 50 nm, the middle parts of the hemicellulose chain had different performances in the two systems, resulting in the peak and plateau area in Figure 5-12 and Figure 5-13 respectively. In the x-positive loading case, the middle parts were stretched. However, in the x-negative loading case, the middle parts were rotated because of the movement of the cellulose bundles. The different performance of the middle parts is the key reason why the two curves in Figure 5-12 and Figure 5-13 are so different. If the chain is rotated, the moving process of the chain is approximately like a rigid body rotation, which would not need too much force or energy. However, if the chain is stretched, the situation is far more complicated. Because the force field

employed is a four-body potential, if an atom is moved away from its equilibrium position, the bond, angle, and dihedral which involves this atom would be changed. The force or energy required is much more than that in the rotation case. That's why there is a flat section in the curve of x-negative loading case.

Therefore, the conclusion of this series of simulations is that the interface strength is affected by the contact area and the structure of the hemicellulose matrices. The more contact area between cellulose microfibril and hemicellulose matrices, the stronger the interface is. Furthermore, unlike the cellulose microfibril bundles, which have a semi-crystalline structure, hemicellulose chain is very flexible. This has been shown in the previous chapter. The hemicellulose chain performs similar to a string with a force applied. If the force is compressive, the string will buckle easily, but if a tensile force is applied, it can be strong despite its flexibility.

CHAPTER 6
MICROFIBRIL ANGLE (MFA) EFFECT

6.1 Introduction to Microfibril Angle (MFA)

The term microfibril angle (MFA) in wood science refers to the angle between the direction of the helical windings of cellulose microfibrils in the secondary cell wall of fibers and tracheids and the long axis of cell (Barnett and Bonham, 2004).

Density has long been considered the main factor of wood quality. However, as Evans and Ilic (2001) mentioned, the influence of MFA on wood stiffness is significantly greater than that of density. They also claim that MFA together with density accounted for more than 95% of the variation in longitudinal modulus of elasticity and that MFA alone accounted for more than 85% of the variation. As the tree grows, the trunk has to be stiffer, or the increasing weight of the tree will break itself. That means mature wood is stiffer than juvenile wood.

It is found that MFA is consistently smaller in latewood cell walls than in those of earlywood in E. nitens (Stuart and Evans, 1994). Since the wood with a larger MFA will have a low Young's modulus, it is only fit for low-grade use. As the forest industry develops, more timber, pulp and wood products are increasingly needed, so that trees are not grown to fully maturity before being harvested. This is why interest is increasing for possible methods to improve wood quality by modifying MFA.

In the following section, simulations are run on various models with different microfibril angles to determine the effect of MFA at the atomic scale.

6.2 MFA Effect

All the models in this part are based on the model with a 0 microfibril angle. The initial structure of the system is shown in Figure 6-1:

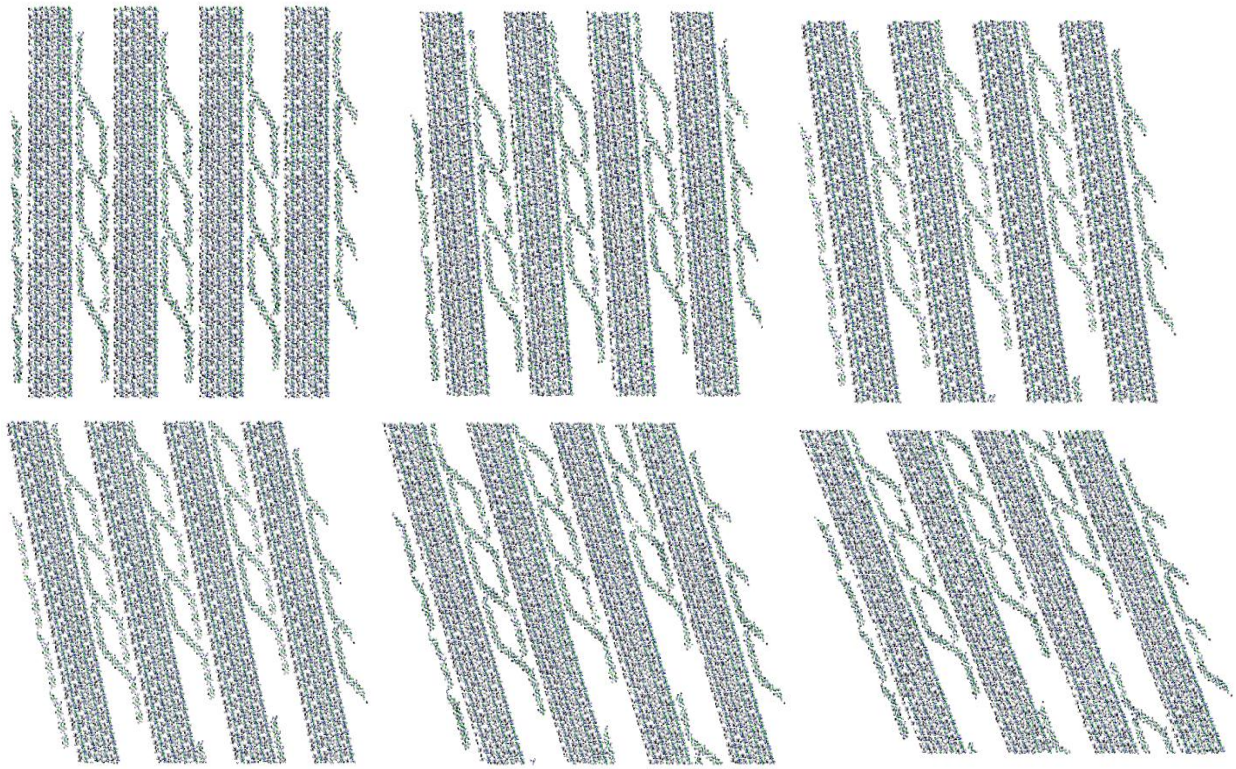

Figure 6-1. Cross-sectional views of one layer in six models. The MFA are 0°, 5°, 10°, 15°, 20° and 25°

The model in the upper left corner is the initial one, which contains four cellulose microfibrils and four groups of z-shape hemicellulose matrices. All these models are put into a periodic box. The bonds, bond angles, and dihedral angles of the models could be across the boundaries of the box, so that the system is actually infinitely huge. Then three stages of relaxation are applied on the six systems. In the first 20,000-step relaxation stage, NVE ensemble was introduced to average the residual stress throughout the system. However, the NVE ensemble could not eliminate the residual stress, so that another 50,000-step relaxation under NPT ensemble was applied to optimize the structure. In addition, the relaxation under NPT ensemble is also a temperature control process. The temperature of the system could be heated up and kept to 300 K. In NPT ensemble, a thermostat and a barostat could control the

temperature and pressure of the system, respectively. Since a compression would be applied on the model, the pressure should not be a constant value. Another 20,000-step relaxation under NVT ensemble was employed for the final optimization. The relaxed structures are shown in Figure 6-2:

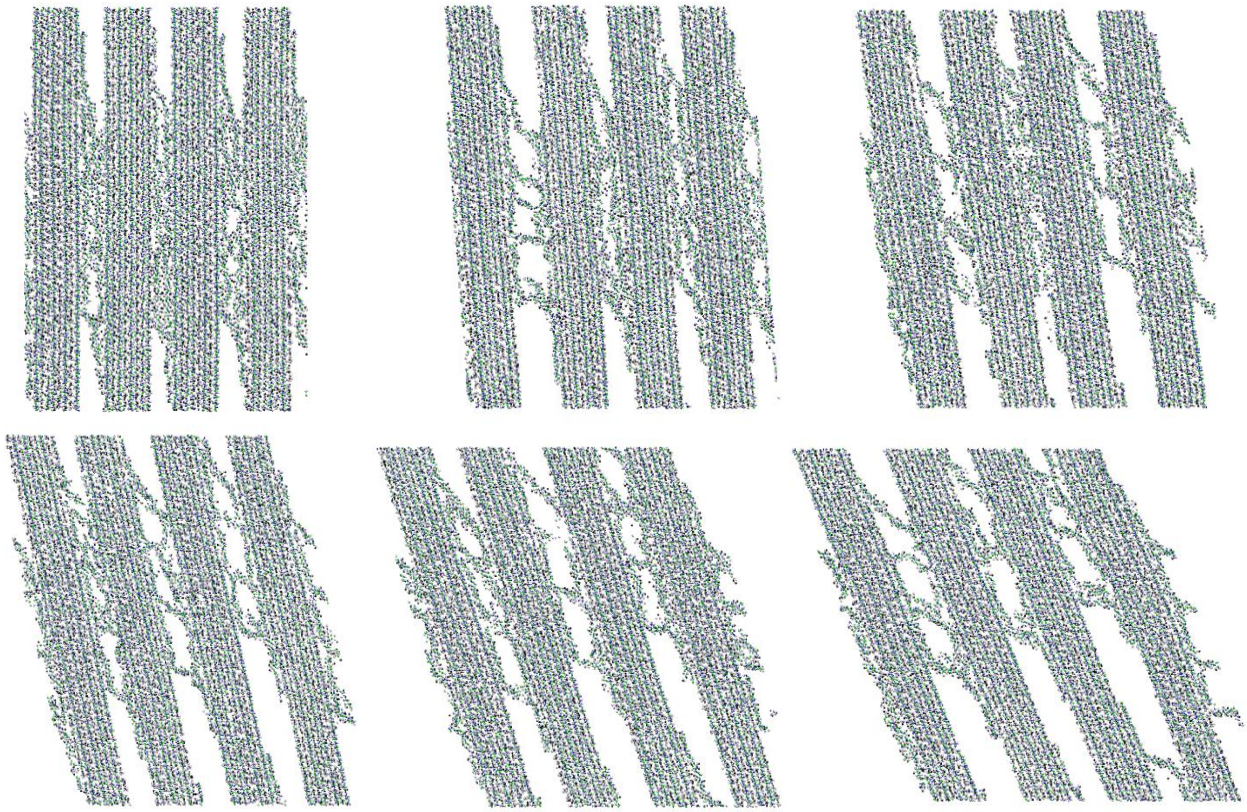

Figure 6-2. Cross-sectional views of the six one layer models after relaxation

After the relaxation, the compression loading is applied on the models. The way we apply the loads is to change the size of the periodic box smoothly. The change in each box is 10% in the y-direction, which is along the axial direction of the cellulose microfibrils in the 0° MFA. The change in the atomic structure is shown in Figures 6-3, 6-4, 6-5, 6-6, 6-7, and 6-8.

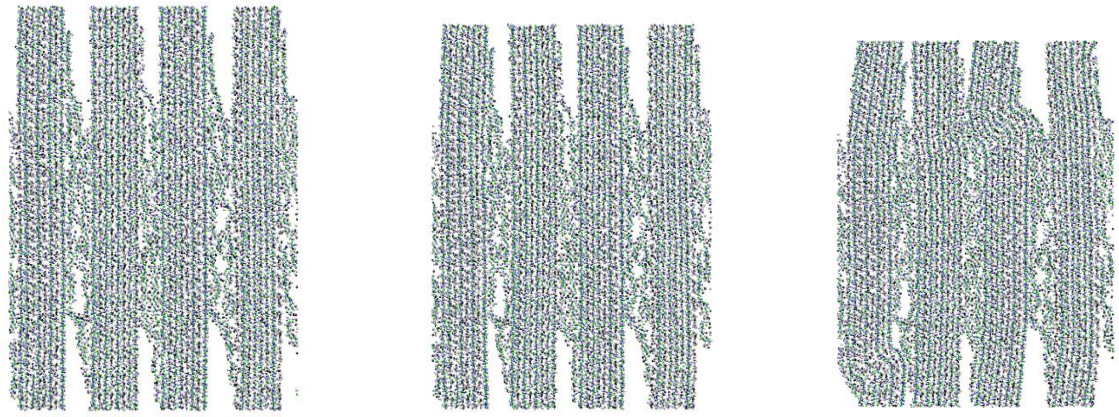

Figure 6-3. Compression process of the model with 0° MFA

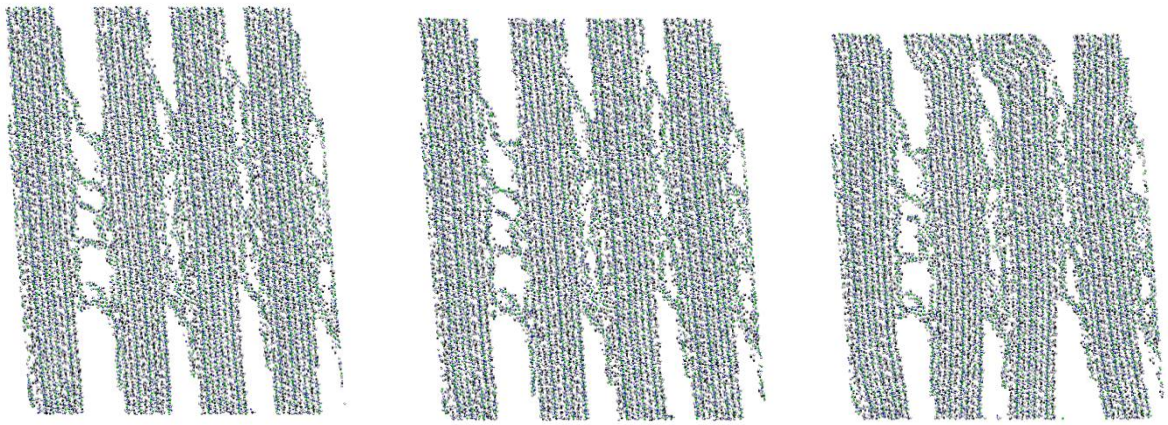

Figure 6-4. Compression process of the model with 5° MFA

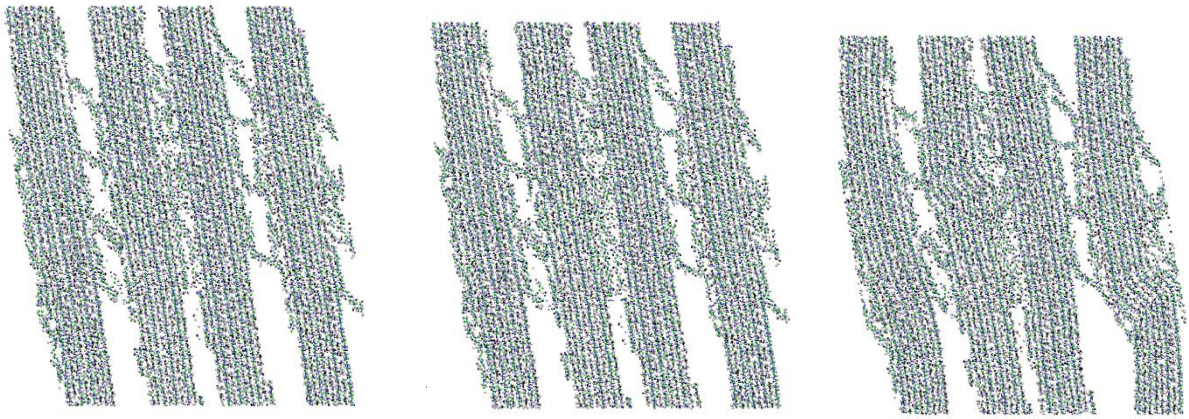

Figure 6-5. Compression process of the model with 10° MFA

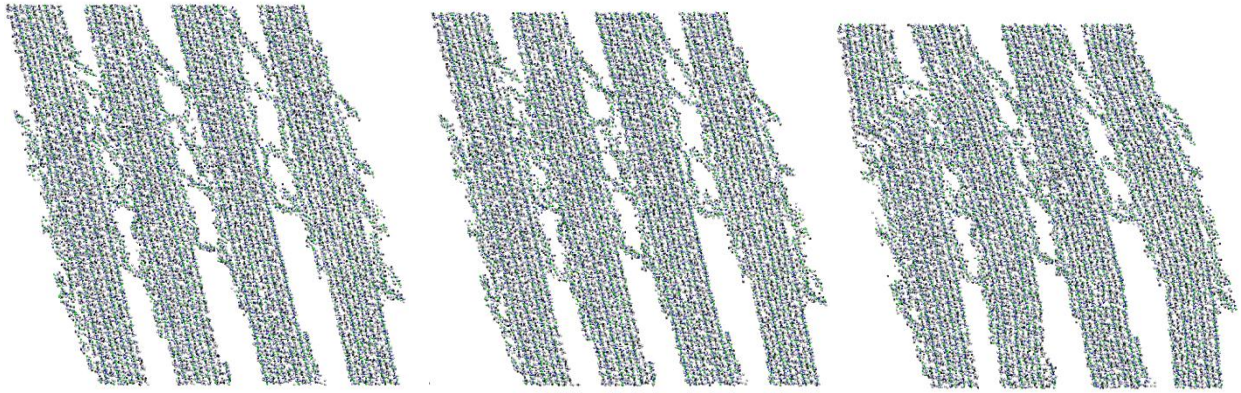

Figure 6-6. Compression process of the model with 15° MFA

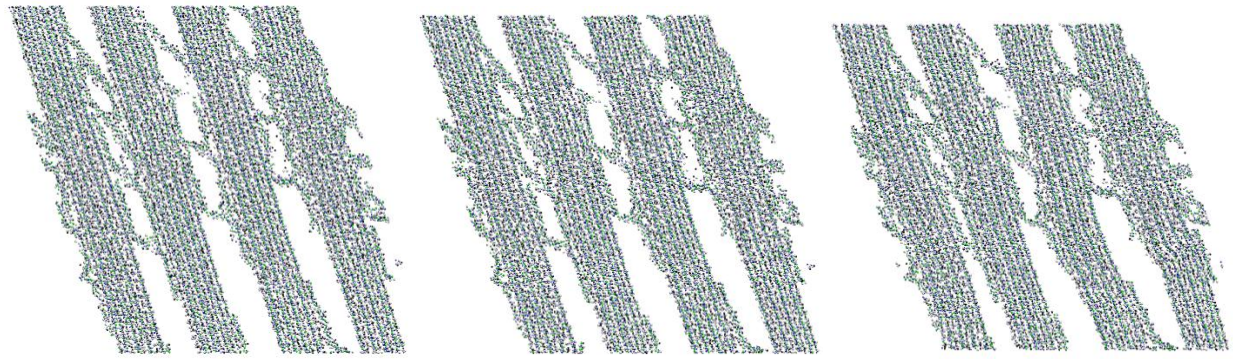

Figure 6-7. Compression process of the model with 20° MFA

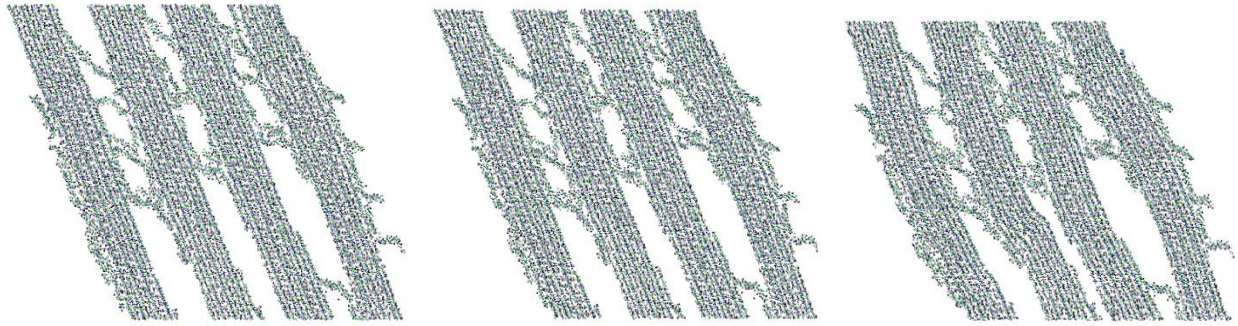

Figure 6-8. Compression process of the model with 25° MFA

Every figure above represents a compression process of a model: the left figures are the initial structure after relaxation, the middle ones represent the elastic deformation of that model, and the right ones show the failure of these six systems. The figures on the right show the buckling occurring on cellulose microfibril. Also, the stress-strain curve of each model is plotted in Figure 6-9.

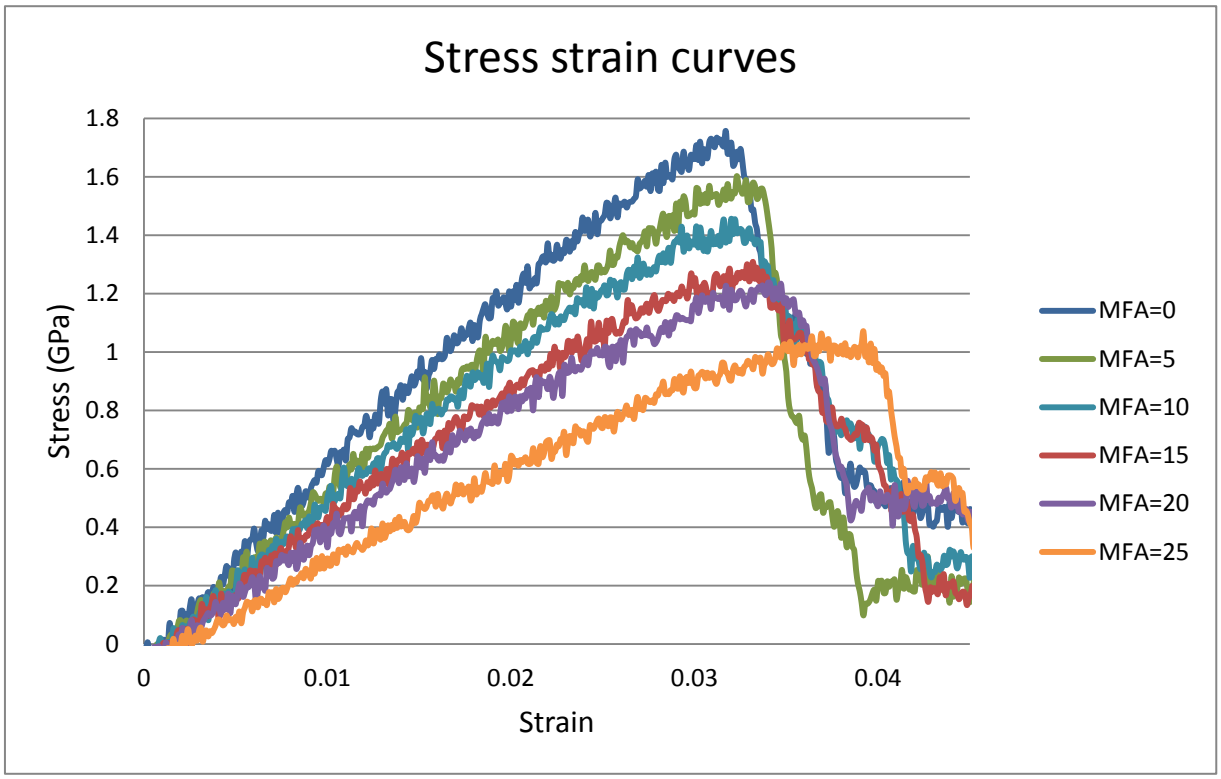

Figure 6-9. Stress-strain curves of six models with various MFA under the same loading rate compression

From the curves in Figure 6-9 the Young's modulus and strength of each model was obtained.

Table 6-1. Mechanical property parameter of six models with various MFA

MFA (°)	0	5	10	15	20	25
Young's Modulus (GPa)	58.974	52.962	49.665	43.841	41.190	32.834
Yield Strength (GPa)	1.76	1.60	1.46	1.31	1.24	1.07
Toughness (MPa)	59.262	55.255	50.857	48.265	47.616	50.454

From Figure 6-9 and Table 6-1, the conclusion could be drawn that the Young's modulus and strength of the system decreases with the increasing of MFA. And the toughness of the system seems to decrease as MFA increases. All of the models failed

due to the occurrence of buckling, and buckling can happen on any part of cellulose microfibril, whether the hemicellulose chains are adhered or not. Therefore, the buckling of cellulose microfibril bundle is the main reason why the systems fail. As the results mentioned in Chapter 5, when the connection between cellulose microfibril bundle and hemicellulose matrices is broken, the deformation of the system is much larger than that of buckling. This means that if the interaction between the cellulose and hemicellulose is broken, the buckling of cellulose microfibril bundle already occurred.

CHAPTER 7
CONCLUSIONS

This paper mainly researches the interactions between cellulose and hemicellulose in the secondary cell wall and the microfibril angle (MFA) effect on the properties of fiber reinforced nanocomposites.

The structural model of cellulose microfibril bundle is generated by using the geometric parameters from experiments. The structure is stable through energy equilibrium. As the periodic boundary condition is applied, the cellulose microfibril bundle has an infinite length.

We also built a model of hemicellulose chain. 4-O-methylglucuronoxylan is the main hemicellulose found in the secondary cell wall of many hardwoods. Xylan and methylglucuronic acid are two main components of this hemicellulose. A unit chain of hemicellulose is built, which consists of six xylans and one methylglucuronic acid.

Various fiber reinforced cellulose-hemicellulose systems based on the models of cellulose microfibril bundle and hemicellulose chain can be designed. In order to explore the interactions between cellulose and hemicellulose, three different hemicellulose matrices are designed. From the results of MD simulation on those three systems, it is found that the more area between cellulose microfibrils and hemicellulose matrices the stronger interactions exhibit. However, contact area is not the only factor affecting the interactions. The shape of hemicellulose chain could also affect the interfacial interactions. During the deformation of the system, if some part of the chain is stretched, more force is necessary to pull the cellulose microfibril bundle away from the hemicellulose matrices. However, if some part of the chain is compressed, this part will

be rotated. Only a small amount of force can depart the cellulose microfibril bundle and hemicellulose matrices.

Furthermore, a study of the microfibril angle (MFA) effect on the properties of fiber reinforced composites based on MD simulation shows the similar result as the experiments observed. The system with a larger MFA has a lower Young's modulus, and the yield strength is not as high as the one with a smaller MFA. The failure of all the systems is buckling. It is also observed that the buckling could be displayed on any part of cellulose microfibril bundle, no matter the adhesive hemicellulose chain lies on it or not. Therefore, we conclude that the buckling of the cellulose bundle is the crucial factor of the failure in the systems. This is related to the structures of the two components: cellulose microfibril bundle has a semi-crystalline structure, while hemicellulose chain is much more flexible. The deformation is very small when buckling appears. However, hemicellulose chain can move some distance with cellulose microfibril bundle before the interaction between them is broken. In other words, if the interaction between cellulose and hemicellulose was broken, the buckling of cellulose microfibril bundle had occurred and the system had collapsed.

LIST OF REFERENCES

[1] T. H. Giddings, D. L. Brower Jr., and L. A. Staehelin, J. Cell. Biol. 84, 327 (1980).

[2] M. C. McCann, B. Wells and K. Roberts, J. Cell Sci. 96,323 (1990).

[3] J.P. Vincken, W. S. York, G. Beldman, and A. G. J. Voragen, Plant Physiol. 114, 9 (1997)

[4] T. Imai and J. Sugiyama, Macromolecules 31, 6275 (1998).

[5] V. L. Finkenstadt and R. P. Millane, Macromolecules 1998, 31, 7776 (1998).

[6] J. F. V. Vincent, J. Exp. Biol. 202, 3263 (1999).

[7] A. Teleman, J. Lundqvist, F. Tjerneld, H. Stålbrand, and O. Dahlman, Carbohydr. Res. 329, 807 (2000).

[8] C. Picard, J. Gruza, C. Derouet, C. M. G.C. Renard, K. Mazeau, J. Koca, A. Imberty, and C. H. D. Penhoat, Biopolymers, 54, 11 (2000).

[9] D. J. Cosgrove, Plant Physiol. 125, 131 (2001).

[10] R. Evans and J. Ilic, For. Prod. 51, 53 (2001).

[11] E. N. Landis, S. Vasic, W. G. Davids, and P. Parrod, Exp. Mech. 42, 389 (2002).

[12] Y. Nishiyama, P. Langan, and H. Chanzy, J. Am. Chem. Soc. 124, 9074 (2002).

[13] D. Kretschmann, Nat. Mater. 2, 775 (2003).

[14] J. Fahlen, L. Salmen, J. Mater. Sci. 38, 119 (2003).

[15] J. Keckes, I. Burgert, K. Fruhmann, M. Muller, K. Kolln, M. Hamilton, M. Burghammer, S. V. Roth, S. Stanzl-Tschegg, and P. Fratzl, Nat. Mater. 2, 810 (2003).

[16] S. J. V. Frankland and V. M. Harik, Surf Sci 505, L103 (2003).

[17] C. Grindon, S. Harris, T. Evans, K. Novik, P. Coveney, and C. Laughton, Phil. Trans. R. Soc. Lond. A 362, 1373 (2004).

[18] J. R. Barnett and V. A. Bonham, Biol. Rev. 79, 461 (2004).

[19] P. Fratzl, I. Burgert and H. S. Gupta, Phys. Chem. Chem. Phys. 6, 5575 (2004).

[20] S. Wan, P. Coveney, and D. R. Flower, J. Comput. Chem. 25, 1803 (2004).

[21] W. Chen, G. Lickfield, and C. Q. Yang, Polymer 45, 1063 (2004).

[22] Z. Xia and W. A. Curtin, Phys. Rev. B 69, 233408 (2004).

[23] D. J. Cosgrove, Nat. Rev. Mol. Cell Biol. 6, 850 (2005).

[24] L. J. Gibson, J. Biomech. 38, 377 (2005).

[25] A. C. Balazs, T. Emrick, and T. P. Russell, Science 314, 1107 (2006).

[26] C. González*, J. Llorca,* Acta Mater. 54*,* 4171 *(*2006*).*

[27] I. Burgert, Am. J. Bot. 93, 1391 (2006).

[28] J. F. Matthews, C. E. Skopec, P. E. Mason, P. Zuccato, R. W. Torget, J. Sugiyama, M. E. Himmel and J. W. Brady, Carbohydr. Res. 341, 138 (2006).

[29] J. Hanus and K. Mazeau, Biopolymers 82, 59 (2006).

[30] S. Ding and M. E. Himmel, J. Agric. Food Chem. 54, 597 (2006).

[31] S. E. Stanzl-Tschegg, Int. J. Fract. 139, 495 (2006).

[32] S. R. Alam, J. S. Vetter, P. K. Agarwal, and A. Geist, Proc. ACM SIGPLAN Symp. Principles and Practice of Parallel Programming (PPoPP), ACM Press 59 (2006).

[33] T. C. Clancy and T. S. Gates, Polymer 47, 5990 (2006).

[34] T. Yui, S. Nishimura, S. Akiba, and S. Hayashi, S. Carbohydr. Res. 341, 2521 (2006).

[35] C. J. Kennedy, G. J. Cameron, A. Šturcová, D. C. Apperley, C. Altaner, T. J. Wess, and M. C. Jarvis, Cellulose 14, 235 (2007).

[36] C. Moine, P. Krausz, V. Chaleix, O. Sainte-Catherine, M. Kraemer, and V. Gloaguen, J. Nat. Prod. 70, 60 (2007).

[37] L. Donaldson, Wood Sci. Technol. 41, 443 (2007).

[38] L. S. Schadler, L. C. Brinson, and W. G. Sawyer, JOM 59, 53 (2007).

[39] M. Bergenstråhle, L. A. Berglund, and K. Mazeau, J. Phys. Chem. B 111, 9138 (2007).

[40] M. E. Himmel, S. Ding, D. K. Johnson, W. S. Adney, M. R. Nimlos, J. W. Brady, and T. D. Foust, Science 315, 804 (2007).

[41] B. Clair, J. Gril, F. Di Renzo, H. Yamamoto, and F. Quignard, Biomacromolecules 9, 494 (2008).

[42] C. M. Altaner and M. C. Jarvis, J. Theor. Biol. 253, 434 (2008).

[43] K. N. Kirschner, A. B. Yongye, S. M. Tschampel, J. Gonzalez-Outeririno, C. R. Daniels, B. L. Foley and R. J. Woods, J. Comput. Chem. 29, 622 (2008).

[44] M. S. Shell, R. Ritterson and K. A. Dill, J. Phys. Chem. B. 112, 6878 (2008).

[45] S. J. Heo, L. Jang, P. R. Barry, S. R. Phillpot, S. S. Perry, W. G. Sawyer, and S. B. Sinnott, J. Appl. Phys. 103, 083502 (2008).

[46] X. Hao, Q. Han and X. H. Yao, Compos. Sci. Technol. 68, 1809 (2008).

[47] Y.Nishiyama, G. P. Johnson, A. D. French, V. T. Forsyth, and P. Langan, Biomacromolecules 9, 3133 (2008).

[48] N. Terashima, K. Kitano, M. Kojima, M. Yoshida, H. Yamamoto, and U. Westermark, J Wood Sci 55, 409 (2009).

[49] T. Yui and S. Hayashi, Cellulose 16, 151 (2009).

[50] Y. Nishiyama, J. Wood Sci. 55, 241 (2009).

[51] D. B. Wells, and A. Aksimentiev, Biophys. J. 99, 629 (2010).

BIOGRAPHICAL SKETCH

Shi Li was born and raised in Wuhan, China. He graduated magna cum laude from Huazhong University of Science and Technology in 2009 with a Bachelor of Science in Mechanical Engineering.

Shi came to Gainesville, Florida in 2009 and was admitted to be a graduate student at the University of Florida's Mechanical and Aerospace Engineering department. He worked with Dr. Youping Chen on his master degree in summer 2010. Shi enjoys reading and exercising.